

# Power Control and Capacity Analysis for a Packetized Indoor Multimedia DS-CDMA Network

Salim Manji, *Student Member, IEEE*, and Weihua Zhuang, *Member, IEEE*

**Abstract**—This paper proposes a packetized indoor wireless system using direct-sequence code-division multiple-access (DS-CDMA) protocol. The indoor radio environment is characterized by slow Rayleigh fading with or without lognormal shadowing. The system supports multimedia services with various transmission rates and quality of service (QoS) requirements and allows for seamless interfacing to asynchronous transfer mode (ATM) broad-band networks. All packets are transmitted with forward error correction (FEC) using convolutional code for voice packets and Bose–Chaudhuri–Hocquenghem (BCH) code for data packets with an automatic retransmission request (ARQ) protocol and for video packets without ARQ. A queuing model is used for servicing data transmission requests. A power control algorithm is proposed for the system, which combines closed-loop power control with channel estimation to give the best performance. Cell capacity of each traffic type and various multimedia traffic configurations in both single-cell and multiple-cell networks are evaluated theoretically under the assumption of perfect power control. The effect of power control imperfection on the capacity using the proposed power control algorithm is investigated by computer simulation.

**Index Terms**—ARQ, capacity analysis, DS-CDMA, FEC, multimedia wireless communications, power control, Rayleigh fading.

## I. INTRODUCTION

RESEARCH and development of wireless personal communication networks (PCN's) are increasingly gaining momentum within the telecommunications industry. Initial services offered by PCN's are limited to voice and low-rate data applications. Future development of PCN's envisions applications for mobile users that extend to a broad range of multimedia services such as voice, data, graphics, color facsimile, and low-resolution video. As a packet-switching technique, asynchronous transfer mode (ATM) is the leading transport mechanism for broad-band networks capable of providing constant, variable, and available bit rate services for multimedia traffic. An extended network consisting of wireless subnetworks to support local users and an ATM network as the backbone for interconnection allows users to have completely tetherless and mobile access to the network for multimedia services. Therefore, it is expected that future wireless networks will be integrated with wired broad-band networks using

ATM technology. The first challenge which arises in the PCN design is to develop a seamless interface between the wireless subnetwork using an error-prone wireless channel and the wired backbone network using a very high-fidelity fiber channel. An important issue is the choice of a suitable radio multiple-access technique capable of providing multimedia services in a protocol compatible with ATM. In this respect, direct-sequence code-division multiple access (DS-CDMA) can offer significant advantages. Different from both frequency-division multiple access (FDMA) and time-division multiple access (TDMA), DS-CDMA accomplishes multiple access by assigning unique spreading code(s) to each user. It can support variable rate traffic by modifying the processing gain or by assigning multiple spreading codes to one user. Since the number of available spreading codes is relatively large as compared with the number of users that can be active at any given time, each base station can assign a code or codes to each new connection as it is established. No additional channel assignment is needed in order for a new user to begin transmission. DS-CDMA is interference limited, therefore, each base station will continue to admit users up to a threshold value at which point the interference causes unacceptable transmission quality. The availability of many spreading codes allows for near perfect statistical multiplexing of the DS-CDMA channel [1]. The network can oversubscribe the channel by making use of statistical multiplexing. Furthermore, in an ATM network, virtual circuit (VC) and virtual path (VP) identifiers located in the packet header allow for unique identification of the source and destination of each transmitted packet. A simple mapping between DS-CDMA spreading codes and VC/VP identifiers removes the need for transmission of this information over the air interface. This can help to simplify routing and to reduce network overheads [2]. A packet DS-CDMA network can provide variable quality of service (QoS) in different ways depending on the traffic characteristics of a particular source, as to be discussed in Section II.

Several system models have been proposed for multimedia and multirate DS-CDMA networks [1], [3]–[7]. The services supported in these models range from one fixed transmission rate to several fixed rates and to true variable rate, and from one QoS requirement to many QoS requirements. Variable spreading gain is one way to provide multiple transmission rates [3], [4]. The inherent drawback is that orthogonal spreading codes are no longer possible; moreover, there is a minimum allowable value of spreading gain in order to maintain the properties of spread-spectrum communications. A system designed to support voice and data services at different transmission rates with a fixed processing gain is discussed

Manuscript received January 18, 1997; revised August 1, 1998. This work was supported by the Information Technology Research Center (ITRC).

S. Manji is with WINLAB, Rutgers, The State University of New Jersey, Piscataway, NJ 08854-8060 USA (e-mail: salim@winlab.rutgers.edu).

W. Zhuang is with the Department of Electrical and Computer Engineering, University of Waterloo, Waterloo, Ont., N2L 3G1, Canada (e-mail: wzhuang@bbcr.uwaterloo.ca).

Publisher Item Identifier S 0018-9545(00)03675-6.

in [5]. However, the system does not support true variable bit rate (VBR) data transmission. A slotted ALOHA model for packet DS-CDMA in a single-cell network is proposed in [6], which is capable of supporting only one variable rate traffic type with a fixed QoS requirement. A network that integrates voice and data transmission is studied in [7]. The model is limited to transmission of information at one fixed rate. An integrated voice/data system that allows for true VBR data traffic is presented in [1], where data sources transmit at the peak channel rate using an ALOHA protocol.

In this paper, we propose a packetized DS-CDMA network model that supports voice, data and video traffic in a protocol compatible with ATM. Bose–Chaudhuri–Hocquenghem (BCH) channel coding is applied to data and video transmission to guarantee a low bit error rate (BER). Different from that proposed in [1], data transmission with a fixed transmission cycle duration is handled by a first-in–first-out (FIFO) queueing system in order to avoid data packet collision. In addition, a reverse link power control algorithm with the best performance is developed for the system operating in a slow Rayleigh fading environment. Through simulation, the performance of the proposed power control algorithm is compared to conventional algorithms in terms of the standard deviation of power control error. The cell capacity of each traffic type and various multimedia traffic configurations in both single-cell and multiple-cell networks is evaluated theoretically under the assumption of perfect power control. The effect of power control imperfection on the capacity using the proposed power control algorithm is investigated by computer simulation. This paper is organized as follows. Section II describes the proposed DS-CDMA multimedia system model that supports voice, data and video traffic in an indoor environment. Section III proposes a power control algorithm for the system, which combines closed-loop power control with channel estimation. In Section IV, the cell capacity for each of the three traffic types and for combinations of the traffic types is studied. Theoretical capacity is evaluated numerically assuming perfect power control, and the actual capacity using the proposed power control algorithm is obtained through computer simulation in order to determine the capacity loss due to power control imperfection. Conclusions of this research are given in Section V.

As there are many variables used in this paper, Table I gives a summary of the important symbols used and their typical value(s).

## II. SYSTEM MODEL

A packetized system model is proposed in the following to accommodate both delay sensitive and error sensitive traffic and to support true VBR services. DS-CDMA is used as the radio channel access protocol. Each base station assigns pseudorandom noise (PN) spreading codes on demand to the mobile users in the cell. For each traffic source, time is segmented into intervals called transmission cycles. Each transmission cycle has a duration  $T_c$ . Each traffic source collects information over the period of one transmission cycle. Information is grouped into fixed length packets. The transmission of a packet starts at the beginning of the next cycle at the peak channel rate  $R_c$ . Since DS-CDMA is interference limited, any burstiness in interference

level will cause substantial degradation in transmission quality for the duration of the burst. Hence, transmission cycles are unsynchronized among users in order to give a distribution of interference closer to uniform than that with synchronized transmission, leading to a higher system capacity. The delay sensitive information with the lowest transmission rate is constant bit rate (CBR) voice requiring a BER of at most  $10^{-3}$ . By incorporating voice activity monitoring, each CBR voice user is modeled as a two-rate source. When a voice user is in talkspurt mode, it generates information bits at a fixed rate,  $R_v$ , and in silent mode, it generates no information bits. The delay between the generation of one bit and the transmission of that bit is approximately the duration of one transmission cycle. Thus, the cycle duration  $T_c$  must be small enough to ensure no distortion in the sound of a voice conversation due to transmission delay. VBR video is another delay sensitive source requiring a BER of at most  $10^{-5}$ . Each video source transmits packets in a method similar to voice sources. It specifies its peak transmission rate to the base station upon the request for admission. If the information generation rate is larger than the peak rate of one CDMA channel, the information is transmitted in parallel over multiple channels by using multiple PN codes so that the transmission delay is not larger than  $T_c$ . For example, if the peak rate of a video source is 1.5 times the peak channel rate, the base station will assign two PN codes to the source. When the actual rate of the video source over the period of one cycle is less than the peak channel rate, it will use only one of its PN codes; otherwise, both PN codes are needed. The system also supports VBR error sensitive data traffic. When a data user has a message ready for transmission, it sends a transmission request to the base station. The traffic is then handled by an FIFO queueing system at the base station after the user is admitted into the system. If the transmission error rates for delay sensitive users are larger than the targeted values, the base station will terminate transmission from some data users in order to reduce interference levels. Details of a connection admission control algorithm for the system are given in [8].

Consider the system with an available bandwidth  $W = 3.2$  MHz and a processing gain  $G = 128$ . Using differential binary phase shift keying (DBPSK) scheme with a bandwidth efficiency of 1.0 b/s/Hz, the peak channel rate is  $R_c = W/G = 25$  kbps, corresponding to a symbol interval  $T_s = 1/R_c = 40 \mu\text{s}$ . For a voice encoder with bit rate  $R_v = 8$  kbps and no forward error correction (FEC) channel coding, the voice user in talkspurt operates on a duty cycle of  $p_a = R_v/R_c = 32\%$ . This is illustrated in Fig. 1(a). The simplest way to make the packetized DS-CDMA compatible with an ATM network is to use a fixed wireless packet payload of 48 bytes after despreading and FEC decoding. Because a wireless channel is highly error prone, the payload should be an integer submultiple of 48 to reduce the probability of packet errors. In this way wireless packets can be easily combined into ATM cells at the connection point between the wired and wireless networks. This provides a relatively seamless interface. In our system model, the payload of each wireless packet is chosen to be 24 bytes as suggested in [9], that is, two wireless packets constitute one ATM cell. With a transmission cycle period  $T_c = 24$  ms, a user in talkspurt mode generates one packet each cycle. When FEC is used, the duty cycle  $p_a$  increases to  $R_v/(R_c r) = (32/r)\%$ , where  $r$  is

TABLE I  
SUMMARY OF IMPORTANT MATHEMATICAL SYMBOLS, THEIR DEFINITIONS, AND TYPICAL VALUE(S)

symbol	definition	typical value(s)
$B_e$	bandwidth efficiency (bits/s/Hz)	
$c_{i,l}$	number of parallel channels used by video user $i$ during frame $l$	
$(E_b/I_o)_q$	required bit energy to interference density ratio (dB)	7.0 (voice), 12.5 (data), 14.5 (video)
$F_m$	inter-cell interference correction factor	0.44 (no shadowing) 0.49 (shadowing)
$f_{Dp}$	maximum Doppler frequency of the pilot link (Hz)	25.2133
$f_{Dr}$	maximum Doppler frequency of the reverse link (Hz)	25.0
$G$	processing gain	128
$I$	interference power	
$k$	number of information bits in the BCH code	192
$L$	number of independent diversity branches	2, 4
$m$	feedback delay factor in power control	
$n$	number of coded bits in the BCH code	224
$N_c$	total number of active mobile users in each cell	
$N_v$	number of voice users in each cell	
$N_d$	number of data users in each cell	
$N_{vd}$	number of video users in each cell	
$P_{b1}$	probability of bit error without retransmission	$10^{-3}$ (voice), $10^{-5}$ (video)
$P_{b2}$	probability of bit error with retransmission	$10^{-6}$ (data)
$p_a$	packet activity factor	0.973 (voice), 0.7467 (data) 0.9856 and 0.5376 (video)
$R_c$	peak channel rate (kbps)	25
$R_d$	data information rate (kbps)	16
$R_v$	voice information rate (kbps)	8
$R_{vd}$	video information rate (kbps)	
$r$	rate of forward error correction (FEC) code	1/3 (voice), 6/7 (data and video)
$S$	normalized received signal power from one user	
$T_c$	period of the transmission cycle (ms)	24 (voice and data), 100 (video)
$T_d$	round trip delay in channel estimation (ms)	
$T_e$	sampling period of channel estimation (ms)	4 (= $100T_s$ )
$T_f$	interval between adjacent video frames (ms)	100
$T_p$	sampling interval of power control (ms)	1.28 (= $32T_s$ )
$T_s$	transmission symbol interval ( $\mu s$ )	40
$u_d$	average number of data users in transmission mode	
$v$	velocity of a mobile user (m/s)	2
$v_a$	voice activity factor	3/8
$W$	available frequency bandwidth (MHz)	3.2
$\beta$	path loss exponent	4
$\Gamma$	average length of each data message (kb)	10
$\lambda_d$	mean message generation rate for data users	
$\mu_r$	normalized average received signal power	
$\phi$	background noise	$\phi/S=1$ dB
$\sigma$	standard deviation of lognormal shadowing (dB)	5
$\sigma_r$	standard deviation of power control error	

the rate of the code. A video user specifying a peak rate  $R_{vdm}$  of less than  $R_c r$  requires only one PN code. For any peak rate higher than  $R_c r$ , the user is assigned  $\lceil R_{vdm}/(R_c r) \rceil$  PN codes (where  $\lceil \cdot \rceil$  is the ceiling function). An example of a video user requiring two PN codes is shown in Fig. 1(b).

It should be mentioned that the choice of packet length has impact on the system performance. The packet length should not be too large, as: 1) for delay sensitive traffic a long packet corresponds to a long transmission cycle which may result in an unbearable transmission delay and 2) for error sensitive traffic an increase of the packet length increases the probability of packet

error and hence the probability of retransmission, resulting in a decrease of the transmission efficiency. On the other hand, a short packet length introduces a relatively large transmission overhead due to packetization. The choice of packet length depends on the characteristics of the communication channel, requirement for transmission accuracy and transmission delay, coding and modulation scheme used, etc. A study on the packet length is given in [10].

The simplest method of accommodating various BER requirements is by adjusting the transmitted power level. Increasing the transmitted power of a user will increase the

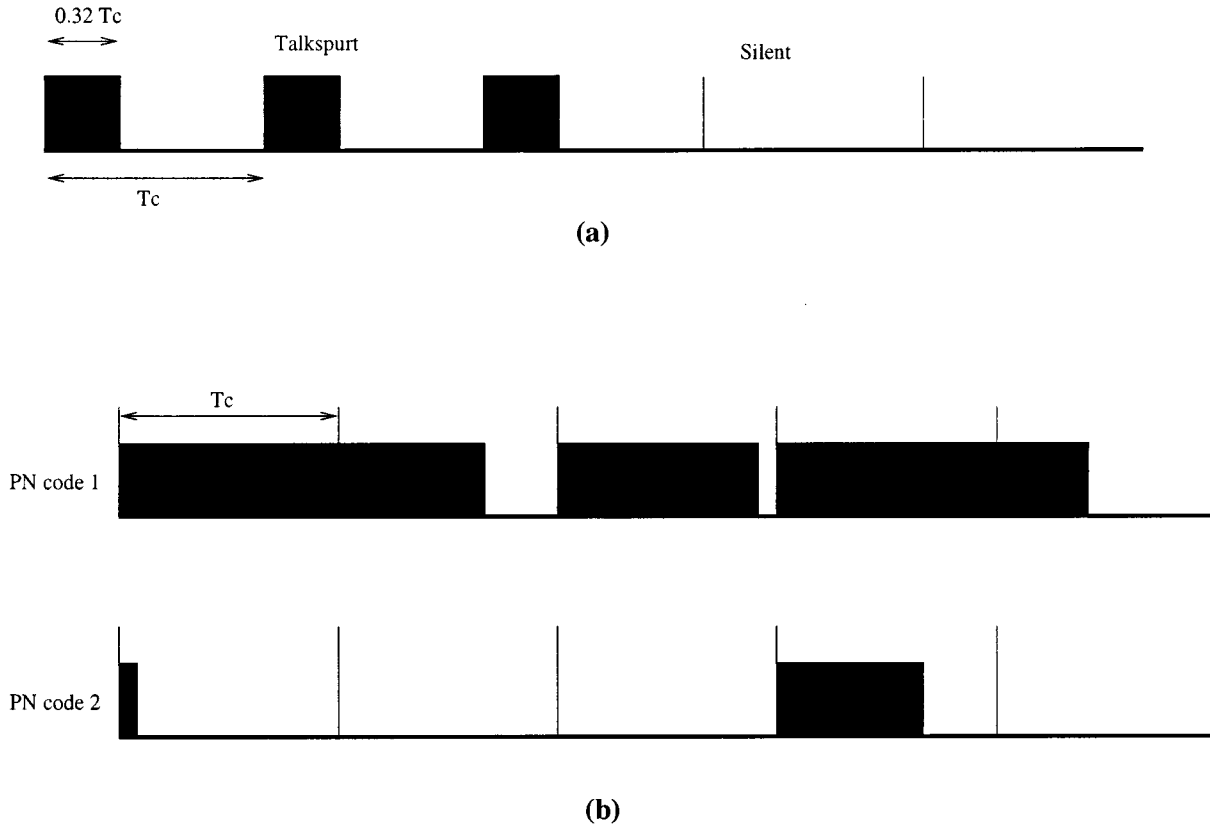


Fig. 1. Transmission cycles of (a) voice user with 32% duty cycle and (b) video user requiring two PN codes.

received signal power, resulting in a larger signal-to-interference ratio (SIR) for that user. SIR can be directly mapped to a corresponding BER, with a higher SIR resulting in a lower error rate. Thus, delay sensitive users with more stringent BER requirements can be accommodated by increasing their transmitted power. The consequence is an increase in the interference seen by all other users in the wireless network. This will increase the BER for all other users or reduce the capacity of the system. In addition, FEC channel coding can be applied to improve the transmission quality. Compared with voice and video users, delay insensitive data users generally require a much lower BER (e.g.,  $10^{-6}$ ), which cannot be achieved simply by increasing their transmitted power. In particular, deep fades of the radio link would require significant transmitted power increases which reduce overall system capacity. Data transmission is fundamentally different from voice and video transmission in that real-time delivery is not a requirement. An alternative is to use both FEC and an automatic retransmission request (ARQ) protocol. This will reduce the BER at the expense of a decreased throughput efficiency because of the required extra coding bits and retransmitted packets. A packet received with more errors than those which can be corrected by FEC coding is considered to be in error. Any packet known to be in error can be retransmitted at some later time in order to satisfy strict BER requirements. An ARQ protocol defines the method of identifying packets in error and the control of retransmission.

FEC coding can reduce the required SIR when the target BER is low, which can then increase overall system capacity and

bandwidth efficiency. Coding is worthwhile if the increase in capacity outweighs the cost of adding redundant coding bits to each packet. A BCH  $(n, k)$  code is considered for data and video transmission, which is capable of correcting up to  $t$  errors or detecting up to  $d_m - 1$  errors in each received packet, where  $d_m \geq 2t + 1$ . We will assume  $d_m = 2t + 1$  in the following. The code can simultaneously correct up to  $t_c$  errors and detect up to  $t_d (>t_c)$  errors as long as  $t_c + t_d < d_m$  [11]. There are three possible fates for each received packet: 1) if the packet has  $t_c$  or fewer errors, the errors are corrected and the packet is successfully received with no bit errors after decoding; 2) if the packet contains between  $t_c + 1$  and  $t_d$  errors, all detected errors cannot be corrected. For data transmission with ARQ, a retransmission request is issued; and 3) if a packet is received with more than  $t_d$  errors, the errors cannot be detected, in which case the packet may be incorrectly decoded as another valid codeword or decoder failure occurs otherwise. The minimum Hamming distance between any two codewords of a binary BCH code is  $d_m$ . If a received codeword is incorrectly decoded, it is most likely decoded to a codeword closest in Hamming distance where, on the average,  $kd_m/n$  of the information bits will be in error. For calculating the BER without ARQ, we will assume (for simplicity of analysis) that a packet with more than  $t_c$  errors will result in a decoder failure, in which case the packet is discarded and all bits are in error. The assumption is reasonable for error sensitive data traffic; however, it is somewhat pessimistic for video traffic as the information can be partially retained in error-tolerant video systems. By assuming any packet with more than  $t_c$  errors results in a decoding failure (the worst

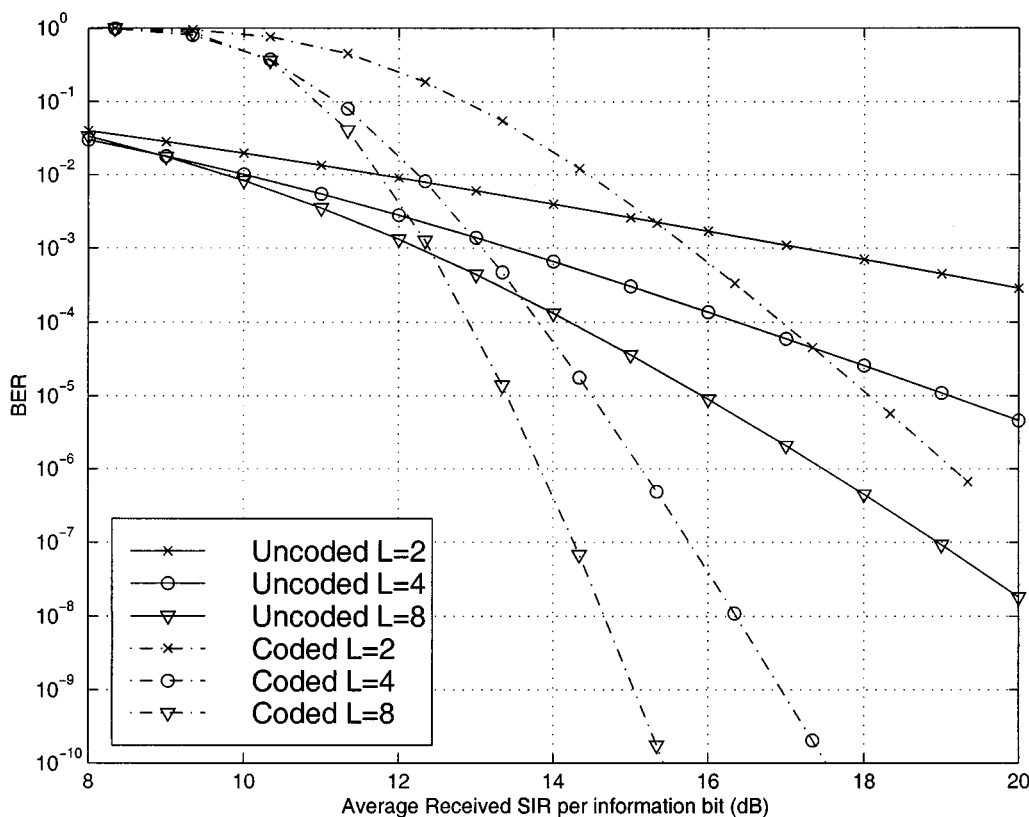


Fig. 2. BER (without retransmission) for BCH-coded DBPSK without retransmission and with  $L$ th-order diversity.

case), the task of finding the BER for coded transmission reduces to finding the probability that there are more than  $t_c$  errors in a packet. Thus, for delay sensitive traffic without retransmission, the BER for a code of length  $n$  in the worst case is

$$P_{b1} = \sum_{i=t_c+1}^n \binom{n}{i} [P_e]^i [1 - P_e]^{n-i} \quad (1)$$

where  $P_e$  is the BER for uncoded DBPSK modulation with  $L$ th-order diversity. It is given in [12] as

$$P_e = \left( \frac{1 - \mu}{2} \right)^L \sum_{k=0}^{L-1} \binom{L-1+k}{k} \left( \frac{1 + \mu}{2} \right)^k \quad (2)$$

where  $\mu = \bar{\gamma}_c / (1 + \bar{\gamma}_c)$  and  $\bar{\gamma}_c$  is the average received SIR per diversity branch. The average received SIR per bit,  $\bar{\gamma}_b$ , is  $L\bar{\gamma}_c$ . For error sensitive traffic with retransmission, the BER needs to be modified accordingly. The probability  $P_s$  of successful reception of a packet is

$$P_s = \sum_{i=0}^{t_c} \binom{n}{i} [P_e]^i [1 - P_e]^{n-i} \quad (3)$$

and the probability of retransmission is

$$P_{rt} = \sum_{i=t_c+1}^n \binom{n}{i} [P_e]^i [1 - P_e]^{n-i}. \quad (4)$$

The probability  $P_d$  of packet error is  $1 - P_s - P_{rt}$  since each received data packet is either successfully received, retransmitted,

or received with undetected error(s). Under the assumptions that: 1) the majority of packets are successfully received and 2) for a packet with undetected error(s) all bits are in error (the worst case), the BER  $P_{b2}$  is approximately equal to  $P_d$ .

In the following, we consider BCH (224, 192) code with  $t = 4$ ,  $d_m = 2t + 1 = 9$ , and  $r = 6/7$ . A lower rate code can further reduce the SIR requirement, but at the cost of more coded bits and a lower processing gain. The rationale for choosing the code (not a lower rate code) is as follows: 1) for video traffic requiring a BER of  $10^{-5}$ , the analysis given in the following shows that the code offers a significant reduction on the required SIR with diversity such as  $L = 4$  and 2) for data traffic requiring a low BER such as  $10^{-6}$ , we rely on ARQ to achieve the target low BER. The high-rate code will correct some (not many) errors and the ARQ is then used to eliminate most other errors. If retransmission were not allowed, then a lower rate code would be desired. Fig. 2 shows the BER ( $P_{b1}$ ) for the BCH-coded and uncoded DBPSK transmission over a Rayleigh fading channel with  $L$ th-order diversity, where retransmission is not allowed. In this situation, error detection is of no utility, thus, we choose  $t_c = t = 4$ . For a fair comparison of BER performance with and without coding, we must consider the effects of coding on the required transmitted power. With a fixed available bandwidth, the coded transmission requires  $1/r$  times the power of the uncoded transmission since the uncoded signal can have a spreading gain  $1/r$  times that of the coded signal. In addition, the required SIR per information bit for the coded signal is  $1/r$  times that for the uncoded signal since the coded signal transmits  $1/r$  coded bits for each information bit. Overall, the coded

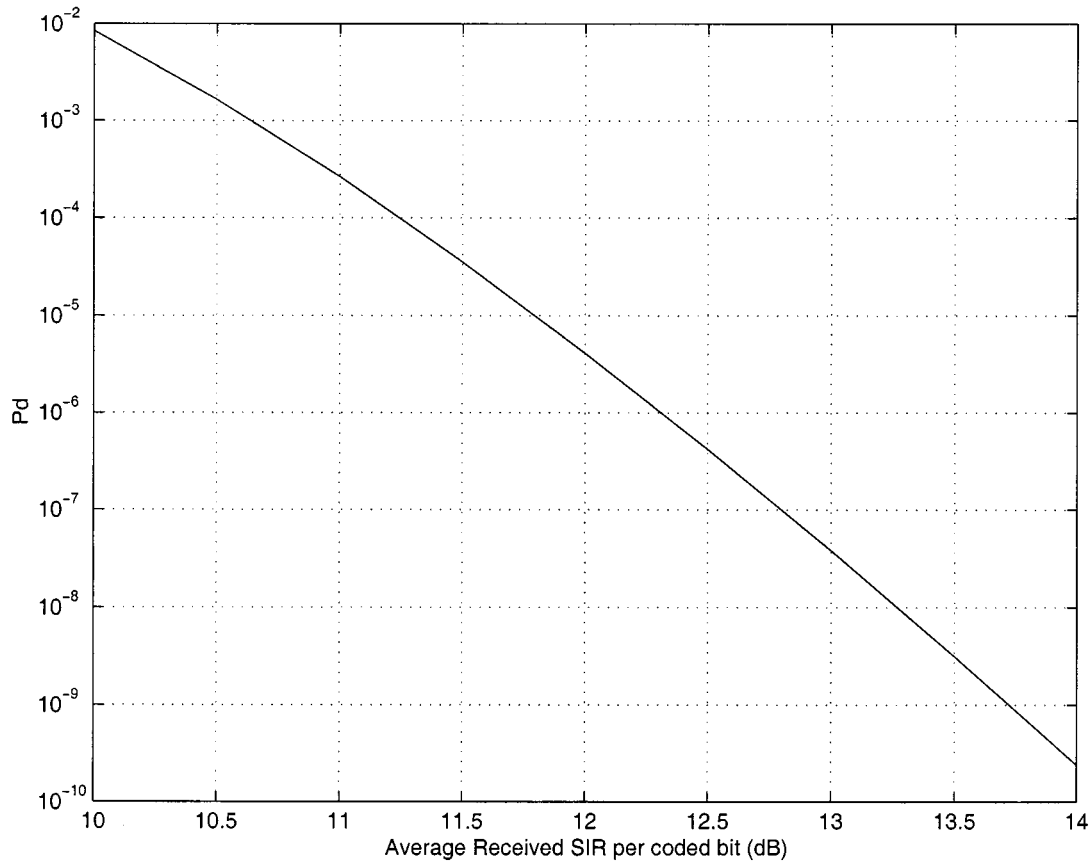


Fig. 3. BER (with retransmission) for data packets using a BCH (224, 192) code with ARQ and fourth-order diversity.

signal requires  $10\log_{10}(1/r)^2 \approx 1.3$  dB more power per information bit than the uncoded signal. From Fig. 2, we can see that the coding scheme reduces the necessary SIR per information bit when the required BER is low. For example, to achieve a BER of  $10^{-5}$  with  $L = 4$ , the SIR requirement falls from 19 dB per information bit without coding to 14.5 dB with coding. That is, the required SIR is  $14.5 - 1.3 = 13.2$  dB per coded bit. For  $L = 8$ , the necessary SIR falls from 16 dB to approximately 13 dB. The benefits of the coding scheme are even more significant as the BER is further reduced. For multimedia systems capable of transmitting data at very low error rates, BCH coding is very useful in reducing the required SIR, thus reducing transmitted power and increasing system capacity. The benefits of BCH coding on data and video packets justify the additional complexity to the system. When the coding is used, the reduction in the required SIR per information bit from  $L = 4$  to  $L = 8$  is not significant enough to warrant the increased receiver complexity. Furthermore, it may not be practical to achieve  $L = 8$  diversity. Fig. 3 shows the BER ( $P_{b2}$ ) taking into account of retransmission. In order to make use of simultaneous error correction and detection, we choose  $t_c = 2$  and  $t_d = 6$ . In a Rayleigh multipath fading channel with  $L = 4$ , an average  $E_b/I_o$  per coded bit of 12.5 dB results in a BER of  $4.18 \times 10^{-7}$  which is slightly better than the target value of  $10^{-6}$ . This corresponds to a retransmission probability of 0.01. Thus, error correction limits retransmissions to a small fraction of packets, causing a negligible reduction in bandwidth efficiency. The low BER requirement is achieved using error detection and ARQ.

For voice transmission requiring a BER of  $10^{-3}$ , as observed from Fig. 2, the transmission performance improved by the BCH code is not significant for  $L = 2$  and 4. A more powerful (lower rate) BCH code or convolutional code should be used. Here, we consider a rate  $r = 1/3$  convolutional code with constraint length 9. The code is also used for the reverse link transmission of voice signals in [13]. Thus, each uncoded voice packet results in  $(1/r) \times 24$  bytes = 576 convolutionally coded bits. The constraint length is the number of memory units required by the decoder plus one. In order for all paths to converge in the decoder, an extra 8-b tail of zeroes is added to the end of each coded packet to effectively reset the decoder back to the initial state. As a result, each coded voice packet has 584 b. With a transmission cycle period  $T_c$  of 24 ms, a user in talkspurt mode generates  $R_v T_c / r = 576$  b plus 8-b tail in one cycle. The duty cycle  $p_a$  for each active user after coding is  $584 / (R_c T_c) \approx 97.3\%$ . The convolutional coding requires a minimum bit energy to interference density ratio,  $(E_b/I_o)_q = 7$  dB [13], in order to achieve a BER of  $10^{-3}$  with noncoherent detection and dual antenna diversity ( $L = 2$ ) for the reverse link transmission.

### III. REVERSE LINK POWER CONTROL

Power control on the reverse link is a key issue in achieving high capacity for the DS-CDMA wireless system. Conventional power control uses an open-loop algorithm, or a closed-loop algorithm, or some combination of the two. Reverse link closed-loop power control for a packetized DS-CDMA network

has been examined in [5] for a system accommodating voice and data users. A closed-loop algorithm based on equal signal strength for data users and on equal error probability for voice users is proposed. The closed-loop power control algorithm in [14] is designed to update the transmitted power of a mobile at a rate faster than that of multipath fading. The received power at the base station is compared to a threshold value and the result is hard quantized to a 1-b power command which informs the user whether to increase or decrease its transmitted power. For the packetized DS-CDMA system model presented in this paper, power control must be reexamined in consideration of packetization and a slow Rayleigh fading channel.

*A. The Proposed Power Control Algorithm*

In general, closed-loop power control may be designed to have a sampling rate that is faster than the rate of multipath fading without the need for excessive feedback overhead. However, a closed-loop algorithm on its own is not sufficient for accurate power control in a packetized network since there may be a large interval between the transmission of consecutive packets. The utility of the feedback information diminishes as the interval between adjacent packets increases. On the other hand, power control can utilize an estimation algorithm to track the current fading state of the channel if the channel fades slowly. This fading state will remain relatively constant over several symbols, thus, the current fading estimate is a useful measure to determine the transmitted power for the next few symbols. Over the reverse link, the proposed power control algorithm makes use of both channel estimation and closed-loop power control. Channel estimation is achieved through the periodic transmission of a reference signal from a mobile to the base station in order to estimate reverse link fading for that mobile. Each mobile transmits a reference signal every  $T_e$  s. The received power of the reference signal at the base station is then fed back to the mobile and is used to determine the transmitted power for the next several symbols. Let  $S$  denote the received signal power from a mobile at the base station. The closed-loop power control is performed by comparing  $S$  with a predefined threshold  $d_t$  over several symbols in order to generate a power control command. The threshold  $d_t$  for each user is determined by its BER requirement because the SIR of the received signal can be directly mapped to a corresponding BER. The control algorithm will feedback a 2-b power command for delay sensitive (voice and video) traffic. The first bit is the output of a comparator with inputs  $S$  and  $d_t$ , and the second bit with inputs  $S$  and  $d_1$  or  $d_2$  depending on the first bit, where  $d_1 < d_t < d_2$ . This results in the following power adjustments:

- if  $S < d_1$ , then increase transmitted power by  $l_1\Delta$
- if  $d_1 \leq S \leq d_t$ , then increase transmitted power by  $\Delta$
- if  $d_t \leq S \leq d_2$ , then decrease transmitted power by  $\Delta$
- if  $d_2 < S$ , then decrease transmitted power by  $l_2\Delta$ .

Here,  $d_1, d_2, l_1$ , and  $l_2$  are design parameters. In the context of the overall performance, it is better to decrease the transmitted power for one user whose received power is above the threshold than to increase the power for one user below the threshold. As

a result,  $l_1 \leq l_2$ . Using  $l_1 = l_2 = 1$  is equivalent to using a 1-b power command. For delay insensitive (data) traffic, only the first bit is used for a 1-b power command. For an indoor environment with a normalized fading rate  $f_{Dr}T_s = 10^{-3}$  (where  $f_{Dr}$  is the maximum Doppler shift in the reverse link), the sampling period of the power control algorithm is chosen to be  $T_p = 32T_s$ , i.e., one power control command for every 32 symbols. In order for the feedback information to be of use, the sampling rate should be faster than the channel fading rate. The algorithm must also allow for a fixed amount of feedback delay, denoted by  $mT_p$  for some integer  $m$ . If we assume  $m = 0$ , the transmitted power for the first 32 symbols at the beginning of each transmission cycle is determined by channel estimation, after which the first power command is generated and the closed-loop control follows. The feedback overhead is 1 b per 16 symbols for voice and video and per 32 symbols for data. Channel estimation generates one estimate of the channel gain  $\hat{a}_p$  every  $N_e (\triangleq T_e R_c)$  symbols.

*B. Performance of Power Control Algorithms*

Voice traffic is considered in the following performance comparison of the power control algorithms based on computer simulation.

1) *Open-Loop Power Control:* Consider a mobile at a fixed distance  $d$  from its home base station using open-loop power control to determine its transmitted power of each symbol. The base station transmits a pilot signal with fixed power  $S_p$  over a slow fading channel. The power of the received pilot signal  $S_r$  at the mobile normalized to  $S_p$  is

$$\frac{S_r}{S_p} = L_p a_p^2 + \frac{S_n}{S_p} \tag{5}$$

where  $a_p$  is the amplitude fading on the pilot link,  $L_p$  is the propagation path loss, and  $S_n$  is the power of the background noise at the mobile receiver. The transmitted power of the pilot signal experiences a path-loss attenuation  $L_p = 10 \log(\xi/10)d^{-4}$ , where  $\xi$  is a zero mean Gaussian random variable with a standard deviation  $\sigma$  of 5 dB for an indoor environment when no line-of-sight path is available [16]. The primary requirement of open-loop power control is to determine the path loss ( $L_p$ ) on the channel. This gives an estimate of the current distance from the mobile to the base station. Fading on the pilot channel causes further fluctuation of the pilot signal. Consider the normalized received signal power of one user. Let the carrier frequency of the reverse link be  $f_{Cr} = 3.75$  GHz, then the maximum Doppler frequency is  $f_{Dr} = f_{Cr}v/C = 12.5v$ , where  $v$  is the velocity of the mobile and  $C = 3 \times 10^8$  m/s is the velocity of light. With  $v = 2$  m/s for an indoor environment, the resulting maximum Doppler frequency is 25 Hz. The normalized fading rate is  $f_{Dr}T_s = 10^{-3}$ . The pilot signal lies in the frequency band of the forward link. Let the carrier frequency of the pilot signal be  $f_{Cp} = 3.782$  GHz, then the maximum Doppler frequency of the pilot link is  $f_{Dp} = f_{Cp}v/c = 25.2133$  Hz and the normalized fading rate  $f_{Dp}T_s$  is  $1.0085 \times 10^{-3}$ . It is well known that power control error resembles a lognormal distribution and that a larger standard deviation results in a smaller actual cell capacity [13], [14], [17]. Ignoring background noise on both pilot and reverse links

and assuming that the distance from the mobile to the base station is fixed, we can evaluate the ability of the open-loop power control algorithm to track fading on the reverse channel based on computer simulation. The simulation is performed by modeling the amplitude fading on the pilot link as a Rayleigh distributed random process with the normalized fading rate  $1.0085 \times 10^{-3}$ . The classical Doppler spectral spread of the Rayleigh fading is simulated using the "sum of sine waves" method [15]. The received pilot signal power is measured over each symbol interval  $T_s$ . The measurement is used to determine the power of the next symbol transmitted on the reverse link. The reverse link is modeled by two paths that fade independently each with the normalized fading rate  $10^{-3}$ . On a logarithmic scale, the standard deviation  $\sigma_r$  of the open-loop power control error is 5.640 dB. The imperfection of the algorithm is due to the fact that the fading and path loss on the pilot channel are different from those on the reverse channel due to the difference in the radio frequency (RF) carrier frequencies and the movement of the mobile.

2) *Power Control Using Channel Estimation:* When fading on the reverse link is approximately constant over several symbols, the base station receiver can estimate the channel fading at one instant and use it for power control over the next several symbols. This is a simple form of closed-loop power control since the base station must periodically feedback to the mobile the information for estimating the channel gain ( $a_r$ ) due to fading on the reverse link. The fading estimator  $\hat{a}_r$  dictates the transmitted power of the mobile. The reference signal from a mobile is received by the base station and is then fed back to the mobile with a roundtrip delay  $T_d$  in order for the mobile to determine  $\hat{a}_r$ . Actually, the power of the received reference signal will include attenuation due to the path loss, channel fading, and background noise on the reverse link. If the distance from the mobile to the base station is relatively constant over the period  $T_e$  of the channel estimation plus the roundtrip delay  $T_d$ , the effects of attenuation due to path loss can be neglected. The channel estimation introduces extra interference into the system due to the transmission of the reference signal. Since the channel fades slowly, the time duration  $T_e$  for each reference signal can be relatively large with respect to the transmitted symbol interval  $T_s$  in order to minimize the added interference and overhead. If the power in the reference signal is fixed for all users, a mobile closer to the base station will cause more interference due to its reference signal. On the other hand, the transmitted power level of the reference signal should be large enough so that a mobile near the edge of the cell will have sufficient power for the reference to be received by the base station because the perturbation of background noise will cause inaccuracy in the channel estimate when the received power of the reference signal is low. The mobile uses open-loop power control to determine the transmitted power for the very first reference signal. Subsequently, the mobile will transmit its reference signal with the same power as that of its most recently transmitted symbol. In this way, the reference signals from mobiles close to the base station will not cause excessive interference. As long as a mobile has not been inactive for a long period of time, this will provide an adequate estimate of the distance from the mobile to the base station. The fading estimate  $\hat{a}_r$  is used to determine the transmitted power for the next  $T_e/T_s$  symbols. Table II shows the

TABLE II  
RECEIVED POWER AND STANDARD DEVIATION WITH  
 $T_e = 100T_s$  FOR THE POWER CONTROL  
USING CHANNEL ESTIMATION

$T_d$	$\mu_r$ (dB)	$\sigma_r$ (dB)
0	0.071	0.778
$10 T_s$	0.093	0.890
$20 T_s$	0.093	1.004
$30 T_s$	0.146	1.117
$40 T_s$	0.117	1.230
$50 T_s$	0.211	1.340

TABLE III  
NORMALIZED RECEIVED POWER AND STANDARD DEVIATION FOR THE  
CLOSED-LOOP POWER CONTROL

$l_1$	$l_2$	$d_1$ (dB)	$d_2$ (dB)	$\mu_r$	$\sigma_r$ (dB)
$\Delta = 0.5$ dB					
1	1	-	-	0.118	0.955
2	3	-0.5	0.5	-0.018	0.520
4	4	-1.0	1.0	0.031	0.537
7	7	-2.0	2.0	0.070	0.703
$\Delta = 1.0$ dB					
1	1	-	-	0.074	0.799
2	2	-1.0	1.0	0.060	0.718
3	3	-2.0	2.0	0.057	0.735
$\Delta = 2.0$ dB					
1	1	-	-	0.179	1.241
$\Delta = 3.0$ dB					
1	1	-	-	0.353	1.782

simulation result of the normalized average received power  $\mu_r$  and the standard deviation  $\sigma_r$  of power control error for various values of the roundtrip delay  $T_d$  with  $T_e = 100T_s = 4$  ms. With a mobile velocity  $v = 2$  m/s, the mobile travels  $vT_e = 8.0$  mm in one interval of  $T_e$ . Therefore, the assumption that the distance from the mobile to the base station is constant over  $T_e + T_d$  is reasonable. In comparison with the open-loop algorithm, the standard deviation of power control error is significantly lower. Even when the roundtrip feedback delay is  $50T_s$ , the standard deviation of power control error is 4.30 dB better than that of the open-loop algorithm. Therefore, channel estimation is more effective in tracking a slow fading channel.

3) *Closed-Loop Power Control:* Closed-loop power control with power commands generated at a rate much higher than the fading rate of the reverse link can be used to further reduce  $\sigma_r$ . The power control sampling period  $T_p$  is chosen to be 1.28 ms, which is comparable to that of 1.25 ms specified in the IS-95 DS-CDMA standard for an outdoor network [18]. A smaller value of  $T_p$  is more effective in tracking the fading and interference in the channel. Choosing  $T_p = 1.28$  ms is a good compromise between low system overhead and accurate channel tracking. This corresponds to  $1/(f_{Dr}T_p) = 31.25$  power control commands per fading cycle on the average. It is assumed that the distance from the mobile to the base station is constant over a duration of sampling period  $T_p$  plus the feedback delay of  $mT_p$ . If the distance changed significantly, then there would be a corresponding change in the path loss. Table III shows the simulation result of the normalized average

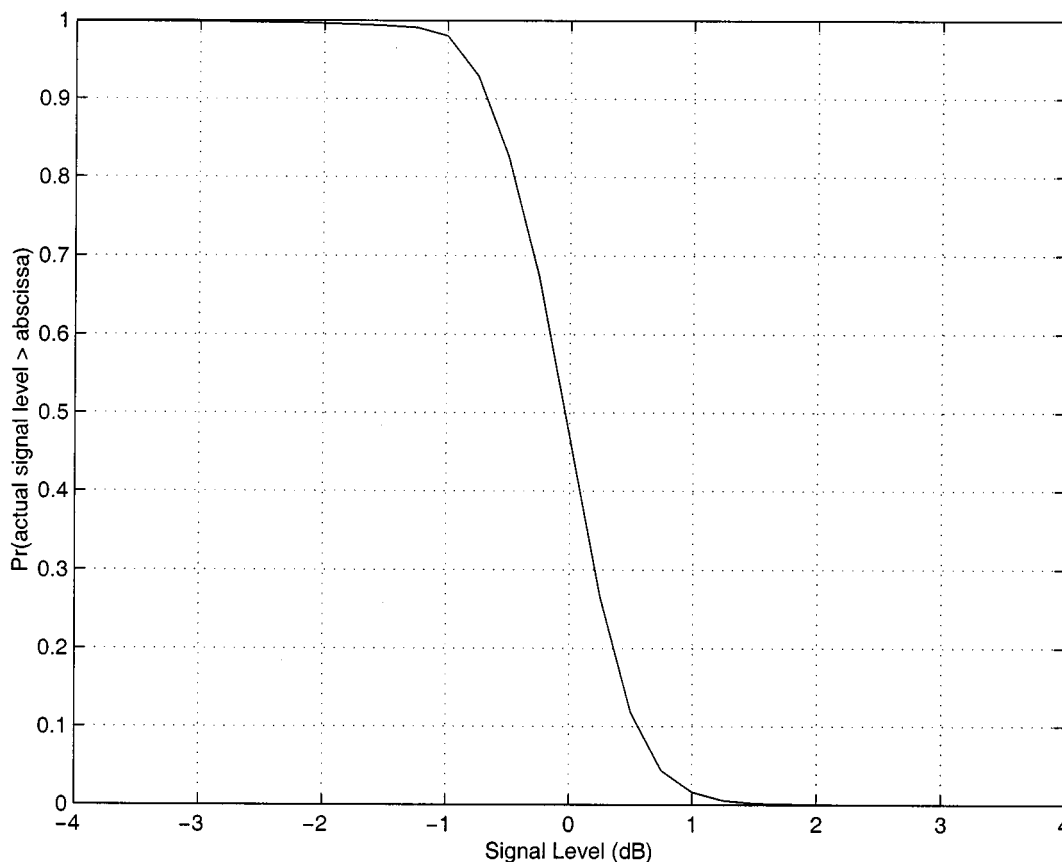


Fig. 4. Power control error distribution for  $(l_1, l_2, d_1, d_2, \Delta) = (5, 6, -1, 1, 0.5)$ .

received power  $\mu_r$  and the standard deviation  $\sigma_r$  of power control error using the closed-loop algorithm with  $m = 0$  and various values of  $l_1, l_2, d_1, d_2$  (dB), and  $\Delta$  (dB). A lower standard deviation directly results in an increased capacity as shown in [17] and [19]. Using a 1-b power command, the lowest  $\sigma_r$  of 0.799 dB is achieved with  $\Delta = 1$  dB. The choice of  $(l_1, l_2, d_1, d_2, \Delta) = (2, 3, -0.5, 0.5, 0.5)$  gives the lowest  $\sigma_r$  of 0.520 dB using a 2-b power command. Fig. 4 shows the simulation result of the power control error distribution with  $(l_1, l_2, d_1, d_2, \Delta) = (2, 3, -0.5, 0.5, 0.5)$ . Approximately 95% of all symbols have normalized received power between  $-1$  dB and  $1$  dB.

4) *The Proposed Algorithm:* Using the proposed algorithm, the channel estimation algorithm is used for the first 32 b in each transmission cycle (assuming a roundtrip delay of  $T_d = 20T_s$ ) and then the closed-loop algorithm is activated for the remaining 552 b of a coded voice packet using a 1-b power command with  $\Delta = 1$  dB and a 2-b power command with  $(l_1, l_2, d_1, d_2, \Delta) = (2, 3, -0.5, 0.5, 0.5)$ , respectively. The closed-loop delay factor  $m = 0$  is assumed. Since the channel fades slowly, only one channel estimate is needed per transmission cycle for each active user, minimizing the added interference due to the reference signals. Computer simulation shows that  $\mu_r$  is 0.071 and  $-0.017$  dB and  $\sigma_r$  is 0.757 and 0.504 dB with 1-b and 2-b commands, respectively.

In summary, the proposed power control algorithm has the best performance among the four power control algorithms. The performance of the closed-loop power control is only slightly

worse than that of the proposed one. In general, the proposed algorithm uses channel estimation at the beginning of each new transmission cycle. If the time gap between adjacent packets increases, closed-loop power control will be less effective on its own as the channel has changed since the last power command was generated, and the performance of the proposed algorithm will further outperform the closed-loop control. The proposed algorithm using channel estimation allows for much more flexibility as the value of  $\sigma_r$  is independent of the time gap between adjacent packets. The flexibility is obtained without much added complexity because channel estimation is a simplified form of closed-loop power control. The cost is the extra interference introduced by the channel estimation.

#### IV. CAPACITY ANALYSIS

For practical closed-loop power control with power control sampling rate  $(1/T_p)$  much higher than the maximum Doppler rate  $(f_{Dr})$  such as the case with  $f_{Dr}T_p \in [0.01, 0.1]$ , it has been shown that the short-term SIR of the received signal generally “fades” as much as the simulated multipath fading itself with diversity, and power control does not provide substantial reduction of the required  $E_b/I_o$  [14]. Therefore, in the following analysis, it is assumed that power control does not change the required  $E_b/I_o$  value in order to achieve a target BER. Perfect power control refers to the situation where the required  $E_b/I_o$  value can be achieved accurately.

### A. Cell Capacity for Voice Users

Consider the capacity of a single-cell network designed exclusively for voice users. Since transmission cycles among users are not synchronized, on the average,  $p_a$  of all active voice users are actively transmitting at any given time. The cell capacity is defined as the maximum number of users such that the required BER is guaranteed for some large fraction of all users at any given time. In order to find the cell capacity, we model each interfering user as a Bernoulli random variable  $\chi_i$  ( $=1$  or  $0$ ) for each transmission cycle. Let  $v_a$  denote the voice activity factor. The event that a user is active during a given transmission cycle is represented by  $\chi_i = 1$  with a probability equal to  $v_a p_a$ . We will assume that  $\chi_i$  during one cycle is independent of all other cycles. Therefore, with perfect power control, the received  $E_b/I_o$  on the reverse link is the same for all users and is given by [13]

$$\left(\frac{E_b}{I_o}\right)_r = \frac{W/R_c}{\left(\sum_{j=1}^{N_v-1} \chi_j\right) + (\phi/S)} \quad (6)$$

where  $N_v$  is the number of users and  $\phi$  is the background noise. For a given user, the outage probability is

$$\begin{aligned} \Pr(\text{BER} > 10^{-3}) &= \Pr((E_b/I_o)_r < (E_b/I_o)_q) \\ &= \Pr\left(\sum_{j=1}^{N_v-1} \chi_j > \delta\right) \end{aligned} \quad (7)$$

where

$$\delta = \frac{W/R_c}{(E_b/I_o)_q} - \frac{\phi}{S}.$$

Since all mobiles transmit independently,  $\sum_{j=1}^{N_v-1} \chi_j$  is binomially distributed with parameters  $N_v - 1$  and  $v_a p_a$ . Therefore, for a given value of  $N_v$ , the outage probability is

$$\begin{aligned} \Pr(\text{BER} > 10^{-3}) &= 1 - \sum_{j=0}^{\lfloor \delta \rfloor} \binom{N_v-1}{j} (v_a p_a)^j \\ &\quad \times (1 - v_a p_a)^{N_v-1-j} \end{aligned} \quad (8)$$

where  $\lfloor \cdot \rfloor$  denotes the floor function. For a cell with parameters  $W/R_c = 128$ ,  $(E_b/I_o)_q = 7$  dB,  $\phi/S = 1$  dB,  $v_a = 3/8$ , and  $p_a = 0.973$ , the theoretical value of the outage probability with perfect power control is shown in Fig. 5(a). To guarantee a minimum required BER of  $10^{-3}$  with a maximum tolerable outage probability of 1%, the single-cell capacity  $N_v$  with perfect power control is 47 users. The bandwidth efficiency  $B_e (=N_v R_v/W)$  is 0.1176 b/s/Hz, which is very close to the single-cell bandwidth efficiency of 0.1256 b/s/Hz given in [13]. In practice, the required BER may be relaxed from  $10^{-3}$  to  $10^{-2}$ , which will lead to an improved cell capacity and therefore a higher bandwidth efficiency. Using the proposed power control algorithm, we will assume that the received power for each interfering user is  $\mu_r$  in the calculation of the outage probability.

Fig. 5(b) shows the outage probability obtained from computer simulation using 1-b and 2-b power commands, respectively. We see that a tolerable outage probability of 1% corresponds to an actual cell capacity of 38 users with a 1-b power command and 41 users with a 2-b power command, corresponding to a 20% and 13% reduction from the capacity with perfect power control, respectively. In other words, the 2-b closed-loop power control algorithm results in an actual single-cell capacity approximately 8% greater than that achieved by using a 1-b power command.

In a multiple-cell network, we must consider the intercell interference from mobile users in other cells in addition to the intracell interference from users within the same cell and background noise. Intercell interference can be stated in terms of an interference correction factor  $F_m$ . Thus, the total interference seen by one user is

$$I = I_c(1 + F_m) + \phi \quad (9)$$

where  $I_c$  is the intracell interference. Under the assumption of no shadowing and full cell loading,  $F_m = 0.44$  [20]. The theoretical value of the outage probability with perfect power control is shown in Fig. 6(a) and the simulation result with imperfect power control in Fig. 6(b). With perfect power control, the cell capacity is 30 users, i.e., intercell interference reduces the cell capacity by 36%. The actual cell capacity is 25 users with a 1-b power command and 27 users with a 2-b power command, corresponding to a 17% and 10% reduction from the capacity with perfect power control, respectively. Thus, the 2-b closed-loop power control algorithm results in the actual cell capacity approximately 8% greater than that achieved by using a 1-b power command.

### B. Cell Capacity for Data Users

For data transmission with FEC and ARQ, the theoretical cell capacity is a function of the average  $E_b/I_o$  which is required to achieve a specified long-term average BER and can be calculated by

$$\left(\frac{\bar{E}_b}{\bar{I}_o}\right)_q = \frac{W}{R_c} \left(\frac{\bar{S}}{\bar{I}}\right) \quad (10)$$

where overbar denotes the average value. For the purpose of calculating the theoretical cell capacity, it is assumed that each data user is a CBR source continuously transmitting at the peak transmission rate  $R_d$  for the duration of the connection. Let  $N_s$  denote the number of such CBR sources. With a packet activity factor  $p_a$  and perfect power control, the average interference is  $\bar{I} = (N_s - 1)\bar{S}p_a + \phi$  for a cell with  $N_s$  data users on the average. That is, the average single-cell capacity is

$$\bar{N}_s = \left(\frac{W/R_c}{(E_b/I_o)_q} - \frac{\phi}{\bar{S}}\right) \left(\frac{1}{p_a}\right) + 1. \quad (11)$$

The maximum number of packets that can be transmitted in one cycle using a BCH code with  $n = 224$  and  $k = 192$  is  $\lfloor R_c T_c/n \rfloor = 2$  packets/cycle. This is equivalent to an actual data information rate  $R_d = 2k/T_c = 16$  kbps. The duty

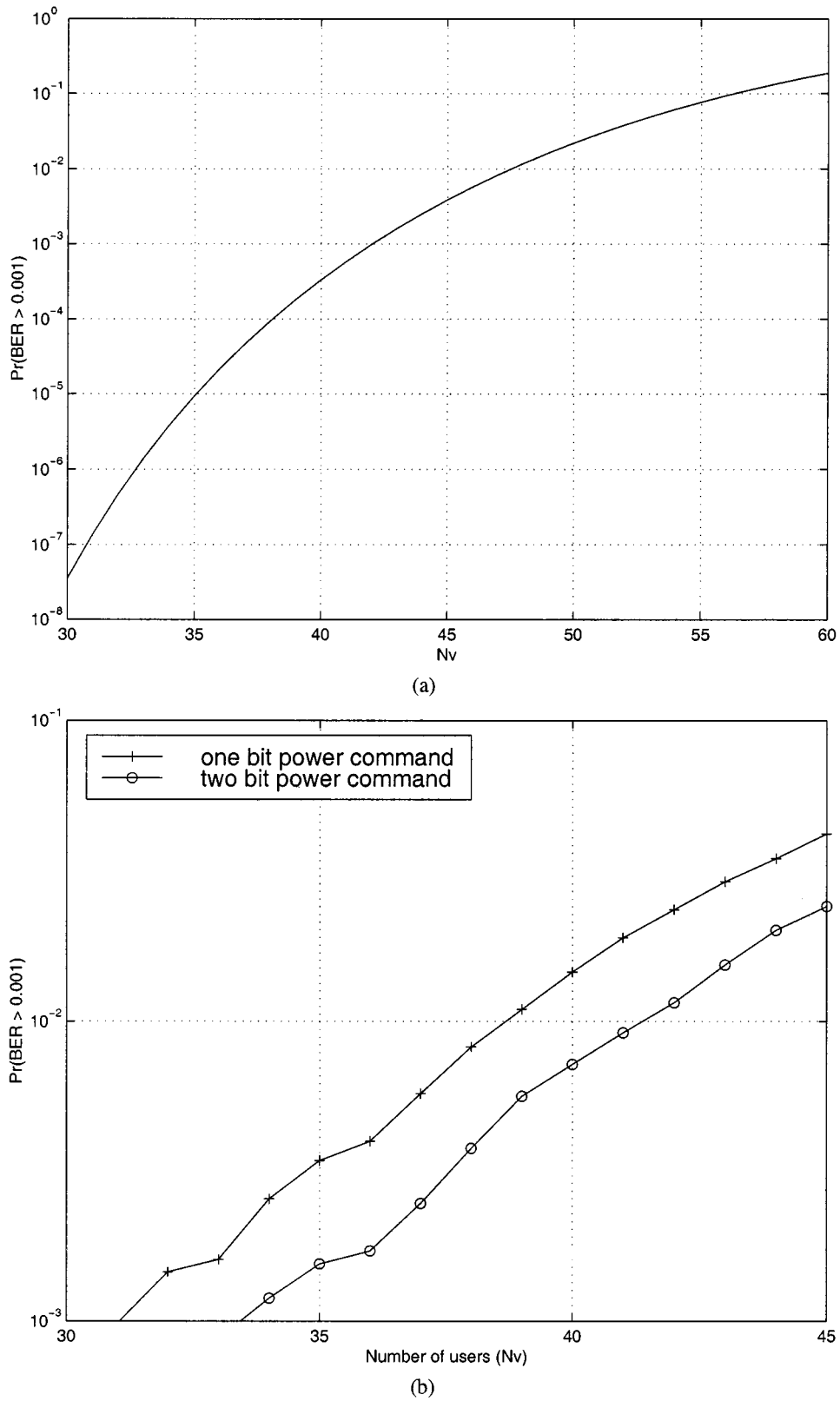


Fig. 5. Outage probability of a single-cell network with (a) perfect and (b) imperfect power control.

cycle for one data user is  $p_a = (R_d/R_c)(1/r) = 0.7467$ . With  $(\overline{E}_b/I_o)_q = 12.5$  dB and  $\phi/S = 1$  dB, the theoretical cell capacity  $\overline{N}_s$  is 8.95 and the bandwidth efficiency  $B_e$  is

0.0448 b/s/Hz for a single-cell network. The lower bandwidth efficiency than that for voice users is due to the much higher transmission accuracy required, i.e., the BER of  $10^{-6}$ .

In the presence of interference caused by other data users and background noise, using the proposed power control algorithm, the received  $E_b/I_o$  per coded bit is

$$\left(\frac{E_b}{I_o}\right)_r = \frac{W}{R_c} \frac{S_d}{(N_s - 1)p_a + \phi} \quad (12)$$

where  $S_d$  is the actual received power per coded bit. Table IV gives the performance of the proposed power control algorithm for data users with  $N_s = 8$ . The results are obtained based on computer simulation with a sample of 400 packets. The performance measures include: 1) the probability that the short-term average (taken over the duration of one transmission cycle) of the received  $E_b/I_o$ ,  $(\overline{E_b/I_o})_s$ , is below 12.5 dB; 2) the long-term average of the received  $E_b/I_o$  (averaged over all 400 packets),  $(\overline{E_b/I_o})_l$ ; and 3) the standard deviation of  $(\overline{E_b/I_o})_s$  from the long-term average. The measure [see 3)] is an indication of the short-term fluctuation of the BER with respect to the long-term average.

The advantage of modeling data users as CBR sources is that we can transfer the results into a queueing model for actual data users generating VBR traffic. In reality, data users are bursty sources. They generate bursts of messages of variable length. Each message is packetized and a request for service is sent to the base station. Requests are queued and serviced by the base station in an FIFO order. With one channel given to each user, the maximum number of requests that can be simultaneously serviced is  $N_s$  with the peak transmission rate  $R_d = 16$  kbps for each user. Under the assumption that the length of each message is exponentially distributed with mean  $\Gamma$  bits, the service time is approximately exponentially distributed. The approximation is due to the fact that each message will be divided into fixed length packets and a small fraction of packets will require retransmission. Let  $N_d$  denote the number of data users (in a cell) each generating messages at a mean rate  $\lambda_d$  messages per second (msg/s). If the interarrival time between requests is also exponentially distributed, an  $M/M/N_s$  queue with mean message arrival rate  $\lambda (=N_d\lambda_d)$  msg/s and mean service rate  $\mu$  msg/s for each server can be used to model the base station handling data source requests. The utilization factor is  $\rho = \lambda/\mu$ , which should be less than  $N_s$  for the queueing system to be stable. Each message is divided into packets of fixed payload length  $k = 192$  b and serviced by one channel capable of transmitting two coded packets per transmission cycle. On the average, a data message will require  $\lceil \Gamma/2k \rceil$  cycles/msg, thus, the mean service time per message is  $\mu^{-1} = \lceil \Gamma/2k \rceil T_c$  s ( $\approx \Gamma/R_d$ ). By ignoring possible packet retransmission, the service time distribution is approximately exponential. Interleaving can be performed over the duration of an entire message since each message is serviced in its entirety by the first available channel. This effectively randomizes bit errors through an entire data message, which allows the BCH code to achieve its full error correcting capability. In summary,  $N_s$  is the maximum number of data channels in the system, each supporting packet transmission continuously in time at the peak rate  $R_d = 16$  kbps. That is, at any given time, the maximum number of data users transmitting packets is  $N_s$ . Due to the bursty nature of data traffic, by using statistical multiplexing, the actual number of data users  $N_d$  that the system can support may be much larger than  $N_s$ , de-

pending on the statistics of data user traffic. This is investigated in the following.

Consider a system with parameters  $\Gamma = 10$  kb/msg and  $\lambda_d = 0.1$  msg/s. The mean information rate for a data user is  $\Gamma\lambda_d = 1$  kbps. This is much less than the peak information bit rate ( $R_d = 16$  kbps) per data channel, therefore, each data user will be serviced by one DS-CDMA channel. On the average, a message requires  $\lceil \Gamma/k \rceil = 53$  packets (i.e., 27 cycles) to complete transmission. The mean service time is  $27T_c = 0.648$  s/msg. The process of message arrivals is Poisson with mean  $\lambda = \lambda_d N_d$  msg/s. For stability, it is required that  $N_d < \mu N_s / \lambda_d (=15.43N_s)$ .

Fig. 7(a) shows the expected number of users in the  $M/M/N_s$  queueing system with  $N_s = 8$ . As  $N_d$  approaches the maximum allowable value of  $15.43N_s$  data users, the average number of users in the system grows exponentially. Fig. 7(b) gives the mean time that a user spends in the queueing system, which is the average message delay. Again, we see an exponential increase as the number of data users approaches the maximum allowable value. For  $N_d < 70$ , the mean time spent in the queueing system is approximately the mean time for services (0.648 s). That is, on the average, a user spends very little time in the queue waiting for service. The optimum value of  $N_d$  depends on several factors. If bandwidth efficiency is of the highest priority, then  $N_d$  should be chosen to be as close to the maximum allowable value as possible. This ensures that all servers are always busy resulting in optimal statistical multiplexing of data traffic. The consequence is excessive queueing delays. Choosing a smaller value of  $N_d$  will reduce bandwidth efficiency and queueing delays. QoS for data users is stated in terms of BER and tolerable data message delay. For example, from Fig. 7(b), a tolerable mean message delay of 1.0 s results in a maximum of  $N_d = 106$  data users in each cell, and from Fig. 7(a) the corresponding average number of data users in the queueing system is 10.47; in addition, it is observed from computer simulation that the average number of servers utilized at any given time is  $u_d = 6.869$ . Let  $P_j$  denote the probability of having  $j$  messages in the queueing system, then the number of busy servers is  $j$  if  $j < N_s$  and is  $N_s$  if  $j \geq N_s$ . As a result, the average number of busy servers is  $\sum_{j=0}^{N_s-1} (jP_j) + \sum_{j=N_s}^{\infty} (N_s P_j)$ , and the average bandwidth efficiency is

$$B_e = \frac{R_d}{W} \left[ \sum_{j=0}^{N_s-1} (jP_j) + \sum_{j=N_s}^{\infty} (N_s P_j) \right]. \quad (13)$$

For  $N_d = 106$ , the bandwidth efficiency  $B_e$  is 0.0343 b/s/Hz, which is 76.6% of the value of 0.0448 b/s/Hz obtained with perfect power control. Table V shows the maximum number of data users ( $N_d$ ) and server utilization ( $u_d$ ) when  $N_s$  servers are available to data sources with a tolerable average message delay of 1.0 s. We can see that  $N_d$  increases approximately linearly with  $N_s (=1, 2, \dots, 6)$ .

In a multiple-cell network, the number of data servers available in each cell can be found by extending (11) to take into account the intercell interference correction factor  $F_m$  as follows:

$$\bar{N}_s = \left( \frac{W/R_c}{(E_b/I_o)_q} - \frac{\phi}{S} \right) \left( \frac{1}{p_a} \right) \left( \frac{1}{1 + F_m} \right) + 1. \quad (14)$$

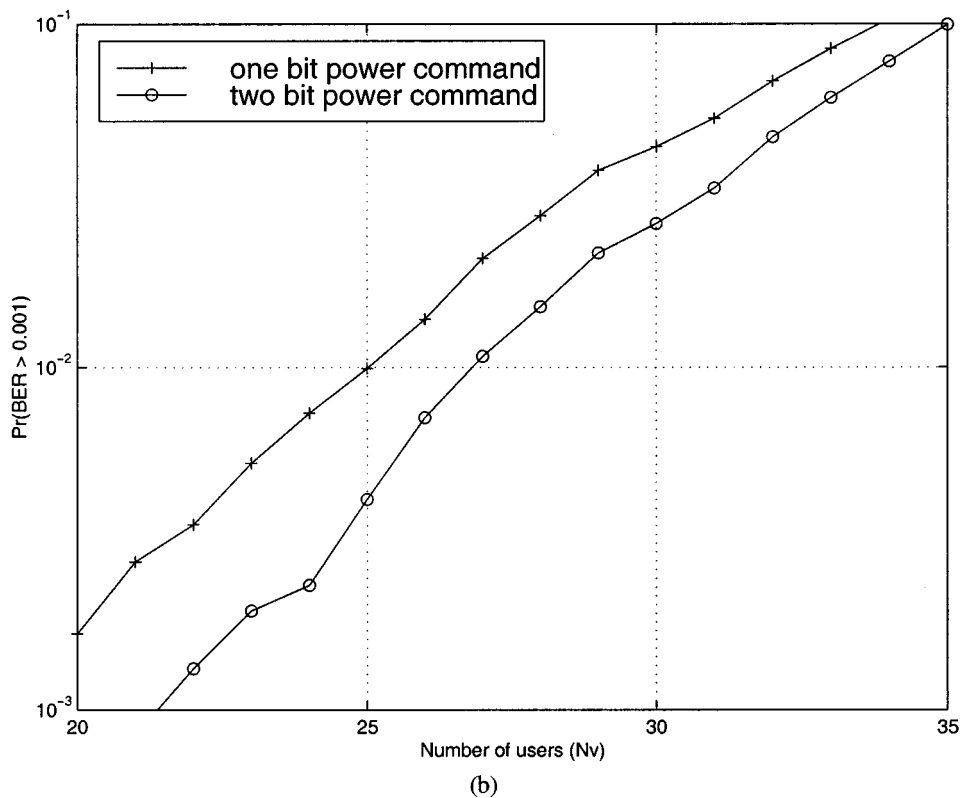
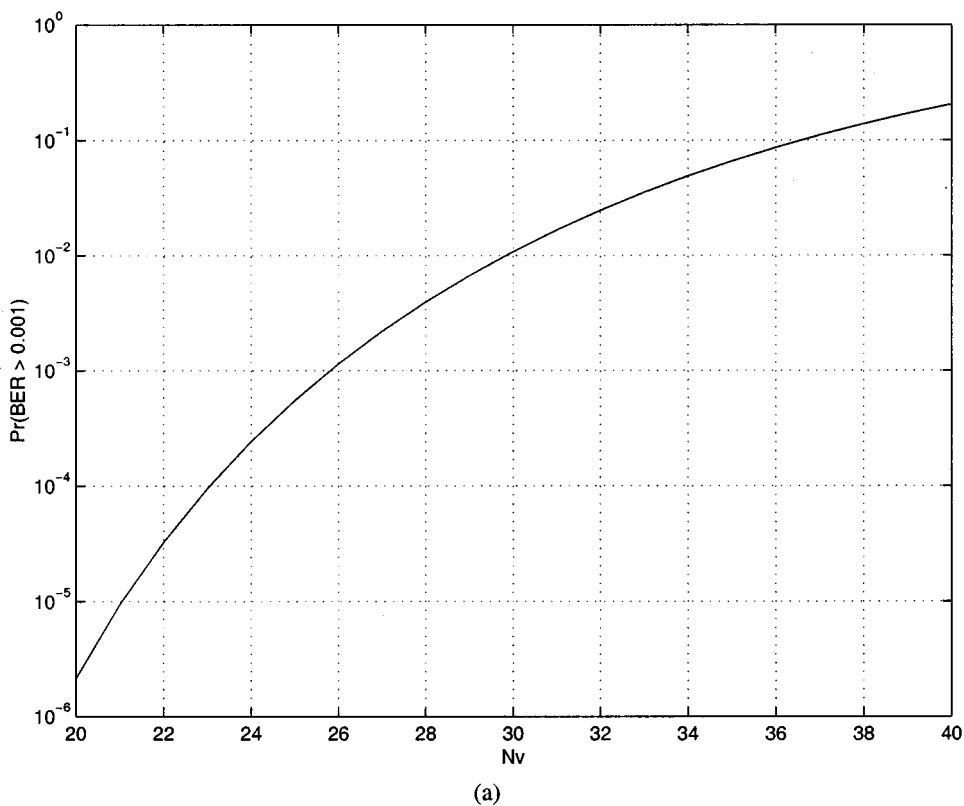


Fig. 6. Outage probability of a multiple-cell network with (a) perfect and (b) imperfect power control.

In [16], shadowing in an indoor environment is characterized as lognormally distributed with  $\sigma = 5$  dB when no line-of-sight path is available. Here, we consider two possible situations for the indoor channel: Rayleigh fading without shadowing, and Rayleigh

fading with lognormal shadowing having standard deviation  $\sigma = 5$  dB. With the control of each mobile limited to the set of the two nearest base stations, a path-loss exponent  $\beta = 4$ , and lognormal shadowing with  $\sigma = 5$  dB, through linear interpolation of the

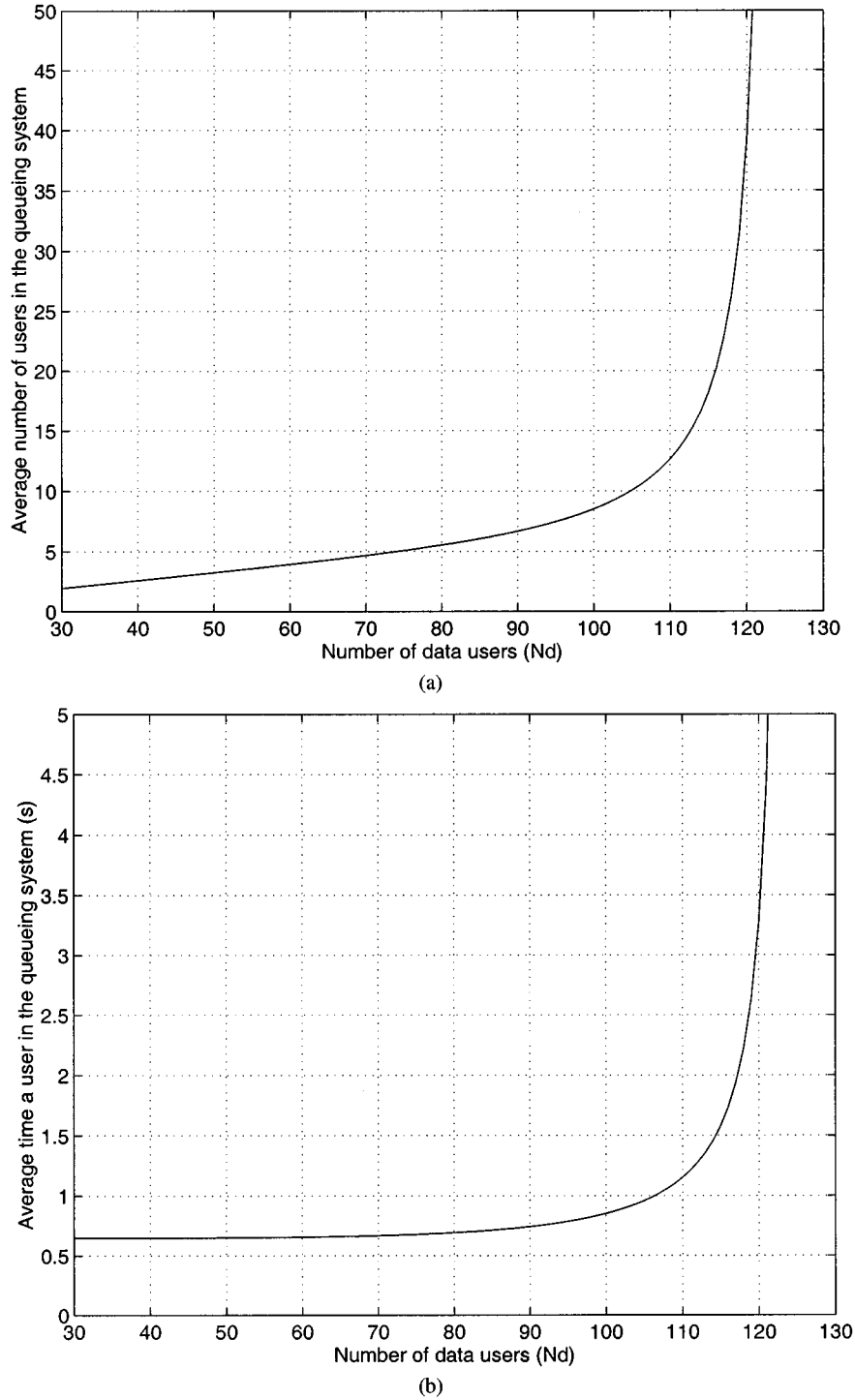


Fig. 7. (a) Expected number of users and (b) mean time a user stays in the queueing system.

results given in [20],  $F_m = 0.49$ . From (14) with  $(E_b/I_o)_q = 12.5$  dB for data users,  $\bar{N}_s$  is 6.52 without shadowing and 6.34 with lognormal shadowing. To study the effect of power control imperfection, Fig. 8 shows the probability that  $(E_b/I_o)_s < 12.5$  dB through simulation with actual power control performed over a sample of 400 data packets. It is observed that the maximum number of data servers is  $\bar{N}_s = 6$  (with 0.5% of probability that the received  $E_b/I_o$  is less than 12.5 dB) and the resulting capacity is  $N_d = 76$  data users per cell.

### C. Cell Capacity for Video Users

Low-rate video with standard  $176 \times 144$  pixels quarter common intermediate format (QCIF) is considered. With the video being scanned at ten frames/s, the interval between adjacent frames,  $T_f$ , is 100 ms. Many codecs have been designed to provide low-rate transmission of QCIF resolution video signals. Video rates as low as 5 kbps [21] have been suggested. We consider a VBR coding scheme with a peak video rate  $R_{vdm}$  of 64 kbps [22]. The two main parameters that characterize the

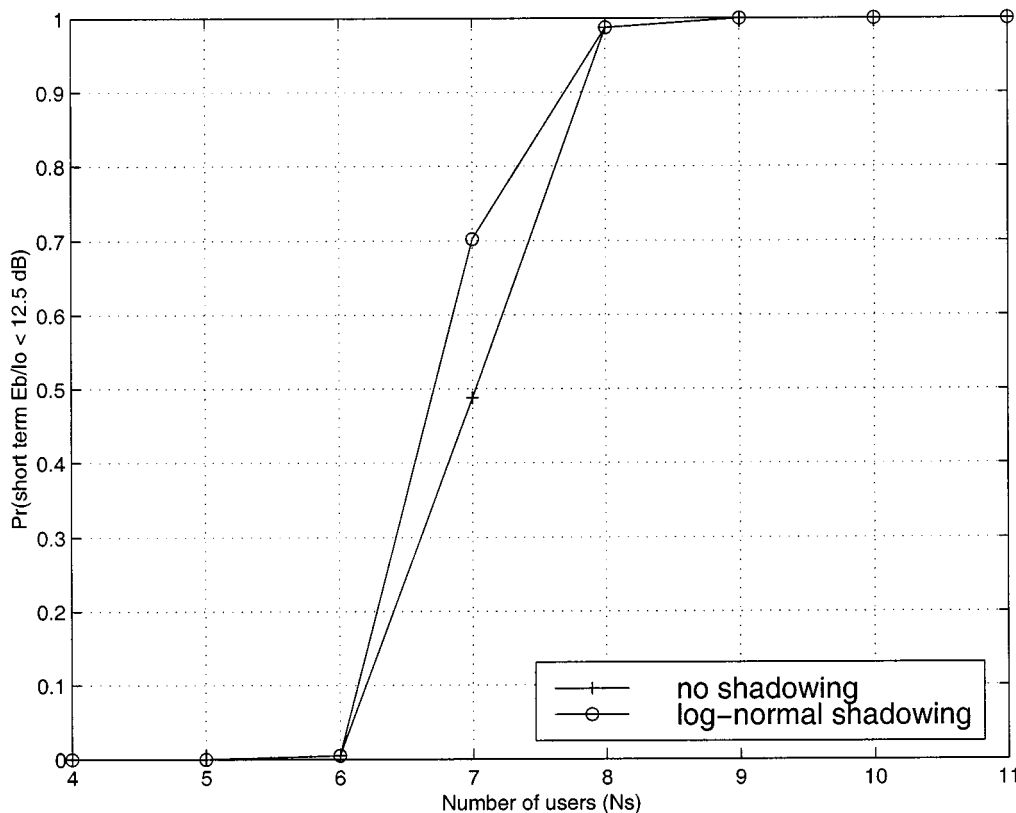


Fig. 8. Probability that  $(\overline{E_b/I_o})_s$  is below the required long-term average in a multiple-cell network.

TABLE IV  
PERFORMANCE OF THE PROPOSED POWER CONTROL ALGORITHM FOR DATA USERS WITH  $N_s = 8$

prob. of $[(E_b/I_o)_s < 12.5 \text{ dB}]$	2.0%
mean of $(E_b/I_o)_l$	13.10 dB
stdv of $(E_b/I_o)_s$	0.275 dB

TABLE V  
MAXIMUM NUMBER OF DATA USERS AND THE SERVER UTILIZATION IN A SINGLE-CELL NETWORK

$N_s$	$N_d$	$u_d$
1	5	0.324
2	18	1.166
3	32	2.074
4	47	3.046
5	61	3.953
6	76	4.925

variability of the video rate are the peak-to-average ratio (PAR) and deviation-to-average ratio (DAR). In [23], it is shown that: 1) low-rate video coding exhibits a PAR of approximately 2.0 and a DAR of 0.3; 2) the distribution is closely modeled by a Gaussian random process; and 3) for applications such as video conferencing, the autocorrelation of the coded information in two consecutive frames can be accurately modeled by a first-order autoregression (AR) process with autocorrelation coefficient  $\rho(T_f) \approx 0.6$  when the scanning rate is ten frames/s.

Using these results, the proposed video coding scheme has a mean video rate  $\bar{R}_{vd} = R_{vdm}/PAR = 32$  kbps and a standard deviation  $\sigma_{vd} = \bar{R}_{vd}DAR = 0.3\bar{R}_{vd}$ . For simplicity, the instantaneous video rate,  $R_{vd}$ , is modeled as a Gaussian random process with distribution  $R_{vd} \sim N(\bar{R}_{vd}, \sigma_{vd}^2)$  and a maximum rate of  $R_{vdm}$ . From Section II, an average SIR of approximately 14.5 dB per information bit or equivalently 13.2 dB per coded bit is required in order to achieve a BER of  $10^{-5}$  using a BCH (224, 192) code with fourth-order diversity. For optimal statistical multiplexing, the transmission cycle period  $T_c$  should be as large as possible. This will effectively spread the transmission of video packets over the maximum duration resulting in an interference distribution that is closest to uniform. The duration of one transmission cycle for video sources will be the duration of one frame,  $T_c = T_f$ . Each active video source will collect the information contained in one video frame. The information is then packetized and BCH coded. Real-time delivery of video signals implies a tolerable frame delay of  $T_f$ . The current frame must be fully transmitted prior to the generation of the next frame. Each video user will generate a maximum of  $(R_{vdm}T_c)/k = 33.3$  packets for one video frame. Using one DS-CDMA channel, the maximum number of packets that can be transmitted in one cycle is  $[(T_cR_c)/n] = 11$ . Thus, each video source requires approximately three parallel DS-CDMA channels in order to transmit at the peak video rate. Because of rounding, the actual peak video rate  $R_{vdm}$  is 63.3 kbps. On the average, a video source will generate  $[\bar{R}_{vd}T_c/k] = 17$  packets per frame. This will require the use of only two of the three assigned PN spreading codes, with the packet activity

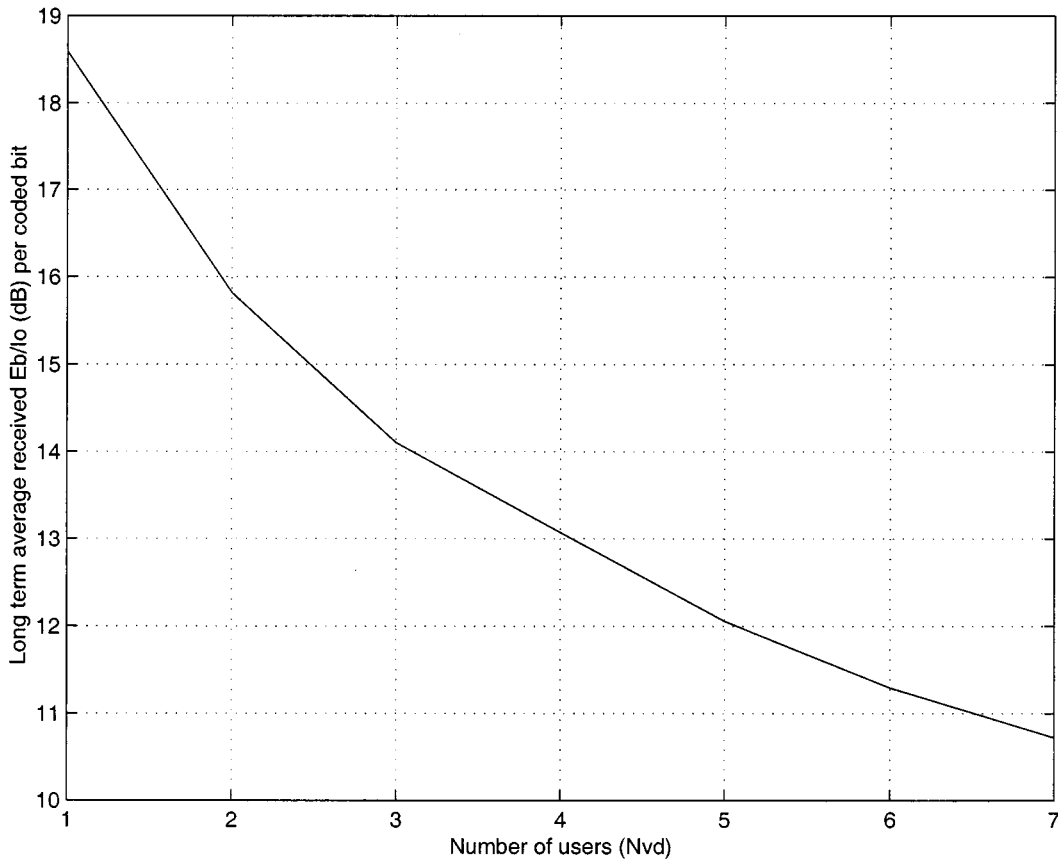


Fig. 9. Long-term average received  $E_b/I_o$  per coded bit.

factor  $p_{a1} = 11n/(R_c T_c) = 0.9856$  on the first channel and  $p_{a2} = (17 - 11)n/(R_c T_c) = 0.5376$  on the second channel.

In order to determine the cell capacity and bandwidth efficiency with perfect power control, we model each active video user as a VBR source. The amount of video information in each frame is Gaussian distributed with mean value  $\bar{C}_f = \bar{R}_{vd} T_f = 3.2$  kb, peak value  $\hat{C}_f = R_{vdm} T_f = 6.33$  kb with the autocorrelation co-efficient of 0.6 in the first-order AR model. With perfect power control, the instantaneous interference seen by user  $i$  during frame  $l$  in a single-cell network with  $N_{vd}$  video users is

$$\begin{aligned} I(i, l) &= \sum_{j=1, j \neq i}^{N_{vd}} c_{j,l} S + I_p + \phi \\ &= \sum_{j=1, j \neq i}^{N_{vd}} c_{j,l} S + (c_{i,l} - 1) S + \phi \end{aligned} \quad (15)$$

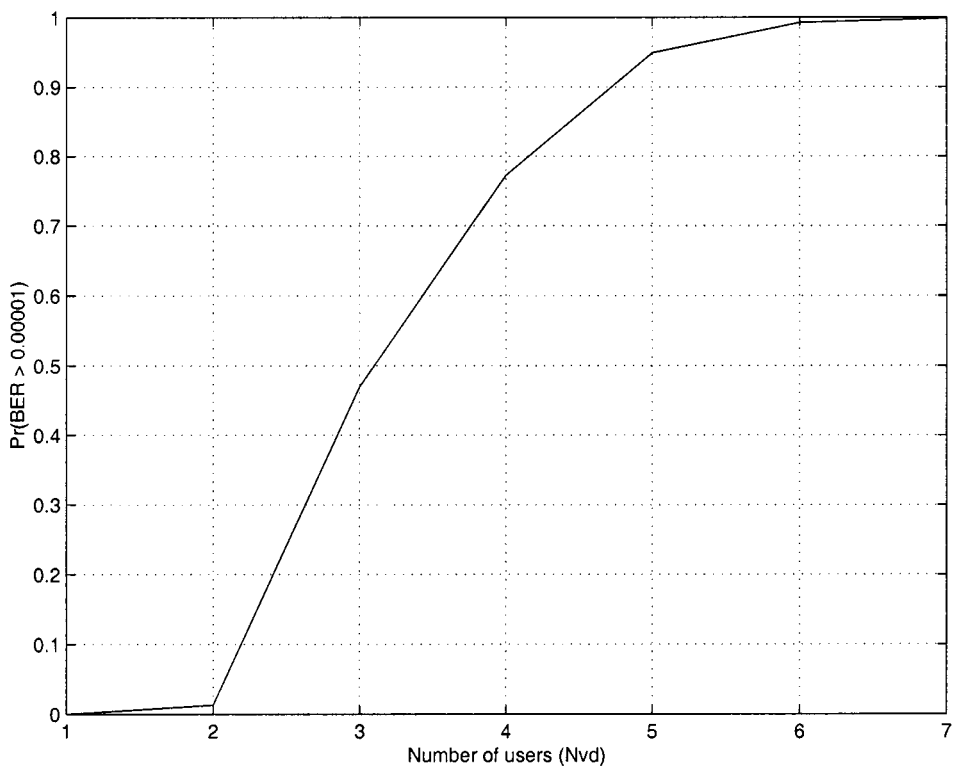
where  $c_{j,l}$  is the number of instantaneous channels in usage by source  $j$ ,  $I_p$  is the interference that user  $i$  causes to its own transmission in each of its parallel channels and is equal to  $(c_{i,l} - 1)S$ . With perfect power control,  $S$  is constant for all users. The received  $E_b/N_o$  is then

$$\frac{E_b}{I_o}(i, l) = \frac{W}{R_c} \frac{1}{\sum_{j=1, j \neq i}^{N_{vd}} c_{j,l} + (c_{i,l} - 1) + \frac{\phi}{S}}. \quad (16)$$

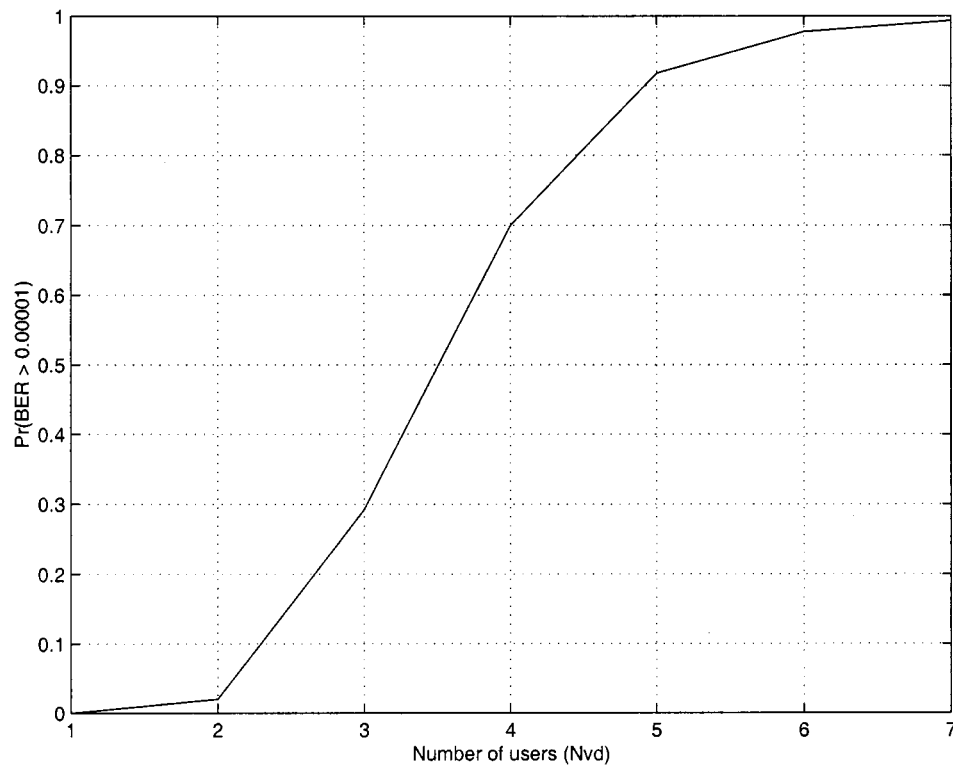
Fig. 9 shows the long-term average of the received  $E_b/I_o$  (averaged over a sample of 100 video frames),  $(\overline{E_b/I_o})_l$ , versus  $N_{vd}$  based on computer simulation. We see that in order to achieve

$(\overline{E_b/I_o})_l$  of 13.2 dB per coded bit, the maximum number of simultaneous video users,  $N_{vd}$ , is approximately 3.9. This results in a BER of  $10^{-5}$  only if the received  $E_b/I_o$  is constant. However, variable video rates will cause interference levels to fluctuate, causing the received  $E_b/I_o$  to change. This will reduce the maximum value of  $N_{vd}$ .

Fig. 10(a) shows the simulated outage probability in a single-cell network with  $N_{vd}$  video users and perfect power control. A received bit is considered to be in outage if its probability of error is greater than  $10^{-5}$ . Thus, the outage can be equivalently stated as the probability that the received  $E_b/I_o$  is below 13.2 dB for a given coded bit. Compared with voice traffic, video transmission may tolerate a higher outage probability. Depending on the video coding algorithm, a bit received in error may degrade the frame quality slightly. The image presented in the frame may contain some misrepresentations, however, the distortion may not be significant enough to render an overall useless picture. On the other hand, VBR video may be run-length coded, in which case a single bit error can result in loss of synchronization and hence in very objectionable artifacts. However, with the target BER of  $10^{-5}$ , the chances of losing synchronization are quite small. From Fig. 10(a), it is observed that when  $N_{vd} = 3$  the outage probability is 47% which is too high to be tolerable; therefore, the cell capacity ( $N_{vd}$ ) under the assumption of perfect power control is two video users (with an outage probability of 1.3%). The bandwidth efficiency  $B_e$  is 0.020 b/s/Hz. This is far below the bandwidth efficiency for voice users because video transmission requires



(a)



(b)

Fig. 10. Outage probability for video users in a single-cell network with (a) perfect and (b) imperfect power control.

a lower BER, thus higher received power. The bandwidth efficiency is also below that for data users. This is the result of the reduced  $E_b/I_o$  requirement for data transmission through the use of ARQ. Next, we will study the transmission of VBR

video traffic using the proposed power control algorithm. In order to estimate the normalized average received power per coded bit for all interfering users, we consider an average frame containing 3.2 kb in which case 17 packets are generated

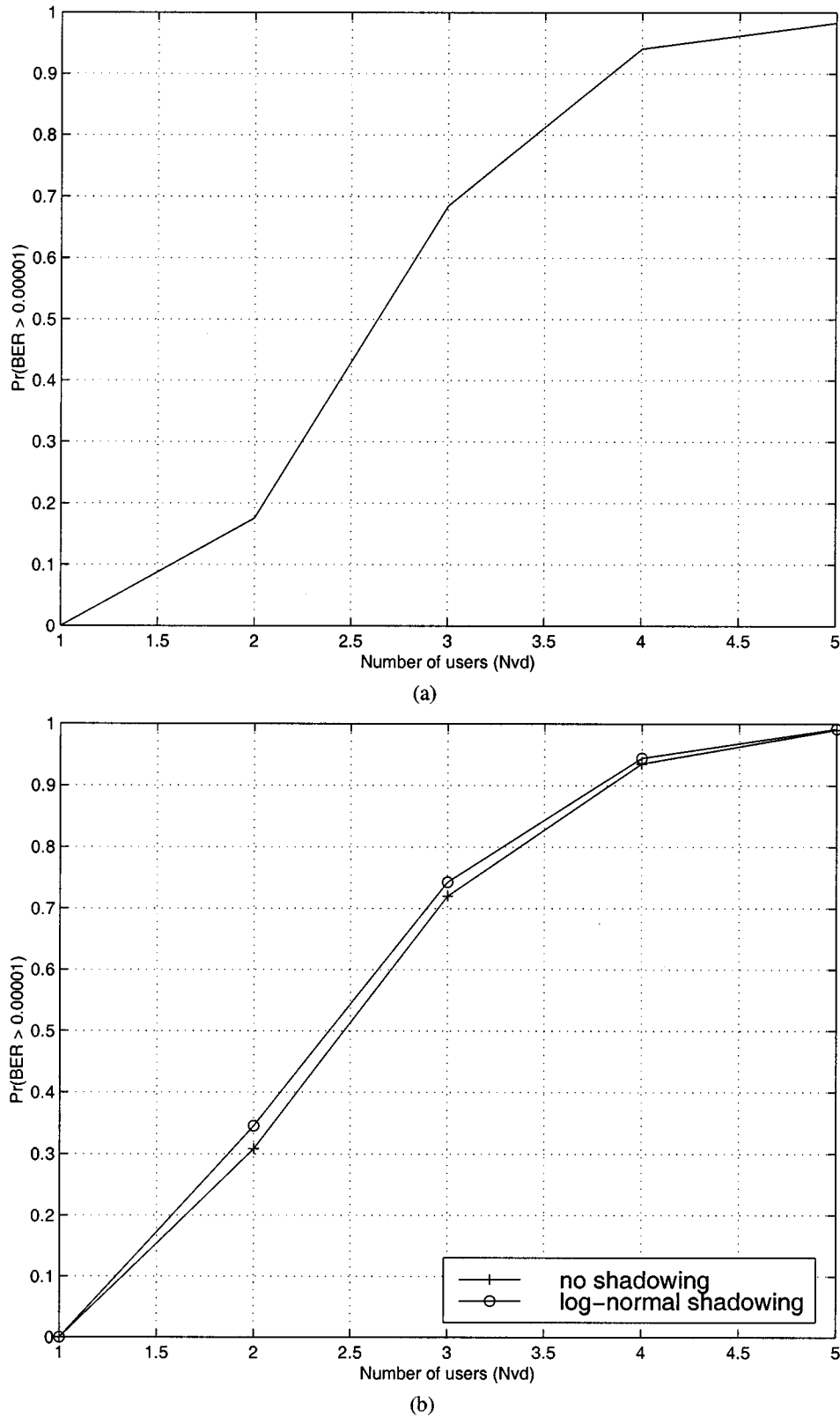


Fig. 11. Outage probability for video users in a multiple-cell network with (a) perfect and (b) imperfect power control.

and two parallel channels are required. The first channel will transmit 11 packets which have  $11n = 2464$  coded bits. The second channel will transmit the remaining six packets which has  $6n = 1344$  b. Channel estimation will control the first 32 b

in each channel and closed-loop power control is used on all subsequent bits. Thus, the estimated average received power per coded bit normalized to  $(\bar{E}_b/I_o)_l = 13.2$  dB is given in the equation at the bottom of the next page. With  $\mu_r$  (channel

TABLE VI  
BANDWIDTH EFFICIENCY  $B_e$  (BITS/S/Hz) AND CELL CAPACITY OF HOMOGENEOUS TRAFFIC IN SINGLE-CELL AND MULTIPLE-CELL NETWORKS, ASSUMING PERFECT POWER CONTROL AND USING THE PROPOSED POWER CONTROL ALGORITHM WITH 2-B COMMAND FOR VOICE AND 1-B COMMAND FOR DATA

traffic type and performance measure		single-cell		multiple-cell	
		perfect power control	proposed power control	perfect power control	proposed power control
voice	$B_e$	0.1176	0.1038	0.0750	0.0675
	$N_v$	47	41	30	27
data	$B_e$	0.0448	0.0343	0.0326	0.0246
	$N_s$	8.95	8.00	6.52	6.00
	$N_d$	118	106	82	76

estimate) = 0.118 dB and  $\mu_r$  (closed loop) = -0.018 dB using a 2-b power command,  $S_e = -0.0157$  dB. The estimated instantaneous interference seen by user  $i$  during frame  $l$  is

$$I(i, l) = \sum_{j=1, j \neq i}^{N_{vd}} c_{j,l} S_e + (c_{i,l} - 1)S(i) + \phi \quad (17)$$

for a single-cell network with  $N_{vd}$  video sources. The added interference  $I_p$  that user  $i$  causes to its own transmission due to the use of multiple parallel channels is  $(c_{i,l} - 1)S(i)$ , where  $S(i)$  is the actual instantaneous received power of the video signal. Fig. 10(b) shows the outage probability using actual power control with a required BER of  $10^{-5}$  based on computer simulation with a sample of 100 video frames. The actual cell capacity is  $N_{vd} = 2$  users, which is the same as the capacity with perfect power control except that the outage probability is increased to 2.0%. With actual power control, the simulated  $(\bar{E}_b/I_o)_l$  is 15.86 dB for  $N_{vd} = 2$ , which is consistent with the perfect power control value of 15.82 dB. For comparison, the system using actual closed-loop power control without channel estimation is also simulated. It is observed that whether the channel estimation is used does not have much effect on the mean and standard deviation of  $(\bar{E}_b/I_o)_l$  and on the outage probability. It is observed from Fig. 10 that the outage probability may be reduced using the proposed power control as compared with the case of perfect power control. This can be explained as follows. Perfect power control implies that the probability of outage is entirely dependent on interference. When interference levels are sufficiently high, a received bit will be in outage. Imperfection in power control will cause fluctuations in the received power, thus, the probability of outage is dependent on both the instantaneous received power and interference. A received bit that is in outage under the assumption of perfect power control may not be in outage when actual power control is used since the instantaneous received power may be above the desired target value.

In a multiple-cell network with perfect power control, the received  $E_b/I_o$  for video user  $i$  during frame  $l$  is

$$\frac{E_b}{I_o}(i, l) = \frac{W/R_c}{\left(\sum_{j=1, j \neq i}^{N_{vd}} c_{j,l} + (c_{i,l} - 1)\right) (1 + F_m) + \frac{\phi}{S}} \quad (18)$$

Fig. 11(a) shows the outage probability for each received coded bit with perfect power control based on simulation with a sample of 100 video frames. The simulation result is independent of whether the lognormal channel shadowing has been taken into account or not. We see that  $N_{vd} = 2$  results in an outage probability of 17.6%, which is likely not tolerable. Therefore, the cell capacity with perfect power control is  $N_{vd} = 1$  video user with a simulated outage probability of 0%. Fig. 11(b) shows the simulation result of the outage probability for video users with actual power control. We see that with  $N_{vd} = 2$ , the outage probability is 30.8% without shadowing and 34.6% with lognormal shadowing, which is too high to be tolerable. Thus, the actual cell capacity is 1 video user.

In the above study of the capacity for video users, the BER requirement of  $10^{-5}$  is considered. However, assuming a more robust video codec which refrains from using run-length coding, the BER requirement could be relaxed to a higher value up to  $10^{-2}$ . This can dramatically improve the capacity for video users.

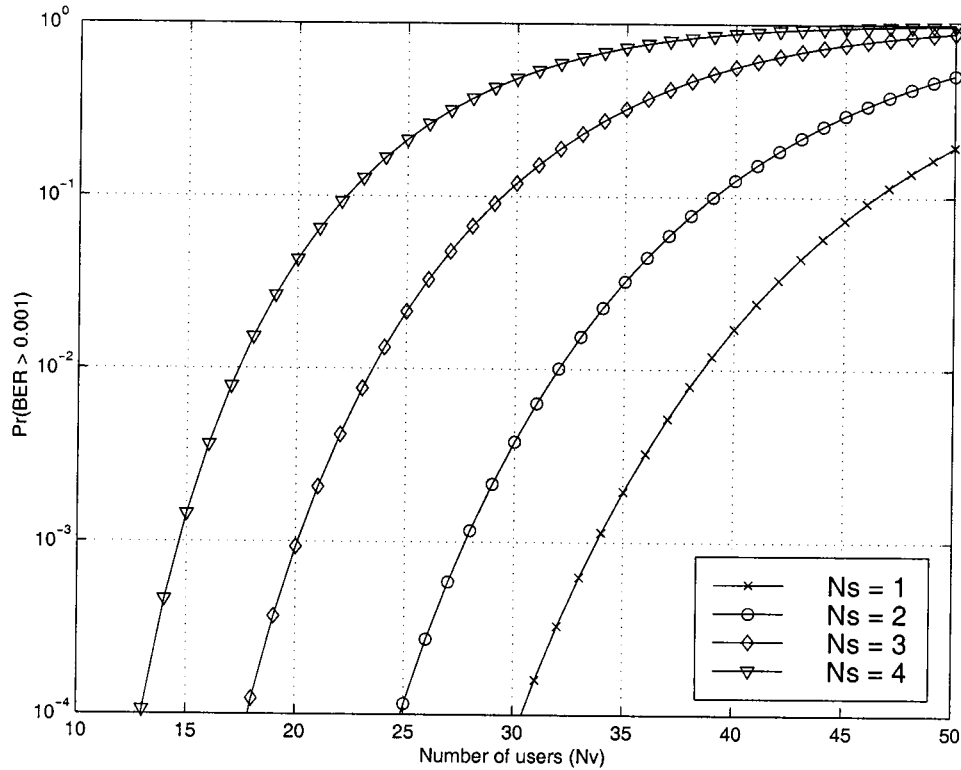
Table VI summarizes the bandwidth efficiency and the cell capacity for homogeneous traffic sources in single-cell and multiple-cell (without shadowing) networks, respectively. Both perfect power control and imperfect power control using the proposed power control algorithm with 2-b command for voice and 1-b command for data are considered. Video traffic is not included because the round error has more effect for the low number of video sources allowed in the networks.

#### D. Cell Capacity for Multimedia Sources

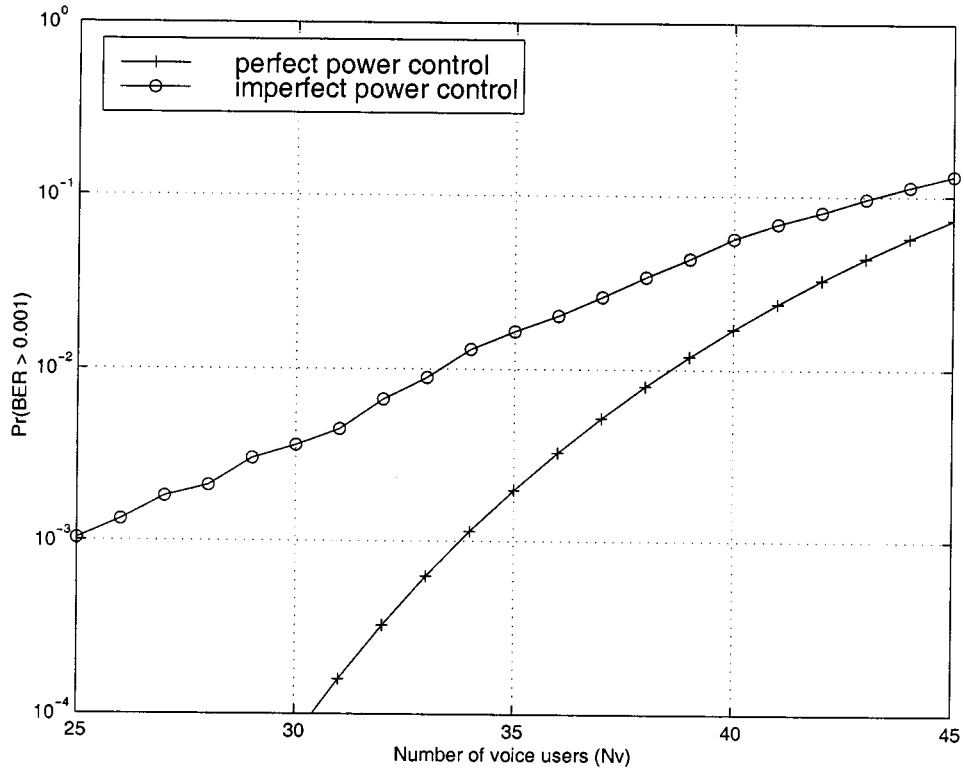
1) *Voice and Data Sources:* In order to integrate voice and data service, we will fix the number of available data servers,  $N_s$ , each corresponding to an active data channel with data rate  $R_d = 16$  kbps, and use all the remaining capacity for voice users. For a given value of  $N_s$ , the interference seen by a voice user in a cell with  $N_v$  voice sources with perfect power control is

$$I(N_s) = \left( \sum_{j=1}^{N_v-1} \chi_j \right) S_v + I_d(N_s) + \phi \quad (19)$$

$$S_e = \frac{(32 + 32)\mu_r(\text{channel estimate}) + (2432 + 1312)\mu_r(\text{closed loop})}{(2464 + 1344)}$$



(a)



(b)

Fig. 12. Outage probability for voice users with (a) perfect power control and (b) imperfect power control ( $N_s = 1$ ).

where  $S_v$  is the power of the received signal from each voice user,  $\chi_j$  is a Bernoulli random variable which is equal to one with probability  $v_a p_a$  (voice) and zero with probability  $1 - v_a p_a$  (voice), and  $I_d(N_s)$  is the interference caused by data users.

The number of data users receiving service at any moment is a random integer in the interval  $[0, N_s]$ . The average number of data users actively transmitting is  $u_d p_a$  (data). We will make the worst case assumption that, at any given moment, all  $N_s$

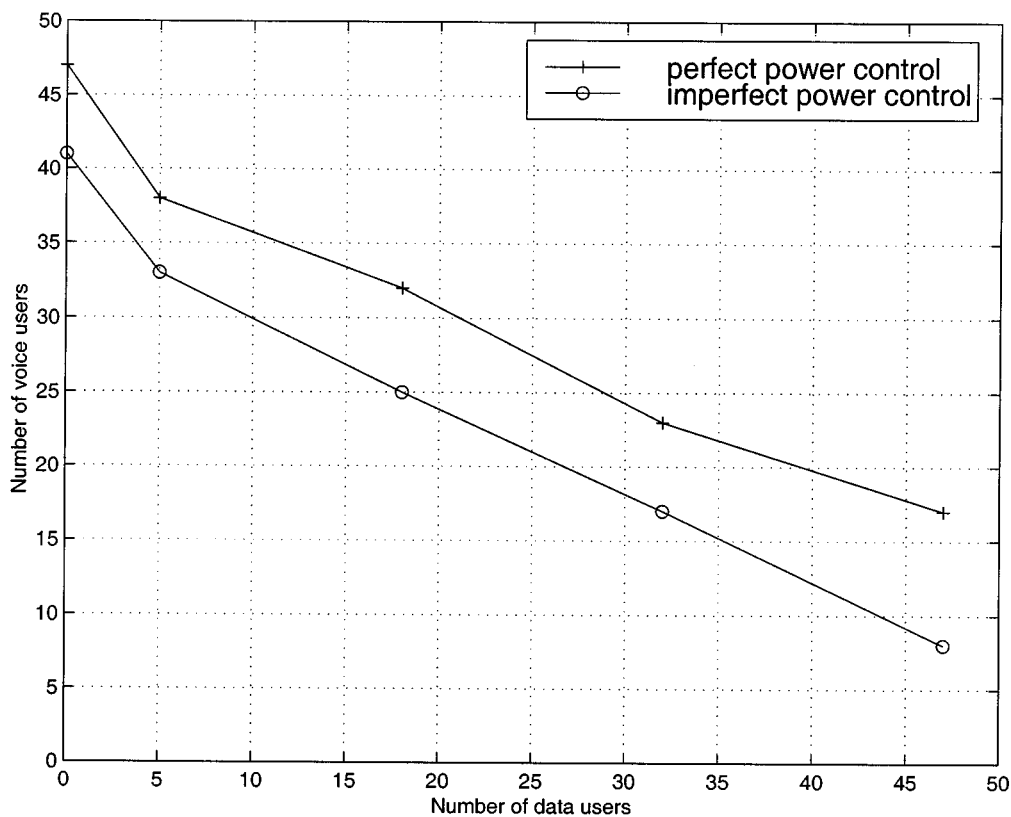


Fig. 13. Number of data users ( $N_d$ ) versus number of voice users ( $N_v$ ).

TABLE VII  
MAXIMUM NUMBER OF VOICE USERS AND TOTAL CELL CAPACITY IN A SINGLE-CELL NETWORK

$N_s$	$N_v$ (perfect)	$N_v$ (imperfect)	$N_c$ (perfect)	$N_c$ (imperfect)	Capacity Loss
0	47	41	47	41	12.8 %
1	38	33	43	38	11.6 %
2	32	25	50	43	14.0 %
3	23	17	55	49	10.9 %
4	17	8	64	55	14.1 %

available data channels are busy. Therefore, the interference caused by the data users is proportional to the actual received power,  $S_d$ , of a data user,  $I_d(N_s) = N_s S_d$ . With perfect power control, the received  $E_b/I_o$  for a voice user is

$$\left(\frac{E_b}{I_o}\right)_r = \frac{W/R_c}{\left(\sum_{j=1}^{N_v-1} \chi_j\right) + \frac{N_s S_d}{S_v} + \frac{\phi}{S_v}} \quad (20)$$

The outage probability for the user is

$$\Pr(\text{BER} > 10^{-3}) = \Pr\left(\sum_{j=1}^{N_v-1} \chi_j > \delta(N_s)\right) \quad (21)$$

where

$$\delta(N_s) = \frac{W/R_c}{(E_b/I_o)_q} - \frac{N_s S_d}{S_v} - \frac{\phi}{S_v}$$

With an  $(E_b/I_o)_q$  of 7 dB for voice users and 12.5 dB for data users, the ratio  $S_d/S_v$  of the received signal powers is 3.548. Fig. 12(a) shows the outage probability for voice users with perfect power control and various values of  $N_s$  based on (19)–(21).

With a tolerable outage probability of 1%, the capacity  $N_v$  for voice users is 47, 38, 32, 23, and 17 for  $N_s$  of 0, 1, 2, 3, and 4, respectively.

Fig. 12(b) shows the outage probability using the proposed power control algorithm for the case of one available data server based on simulation. As expected, power control imperfection reduces the actual cell capacity. The capacity  $N_v$  for voice users reduces from 38 with perfect power control to 33 with imperfect power control. Fig. 13 shows the number of data users versus the number of voice users in a single-cell network. We see that there is a linear relationship between the capacity for voice users and that for data users, and one data user is approximately equivalent to 0.6 voice users in terms of the total single-cell capacity. It should be mentioned that the nonlinearity at  $N_d = 5$  (or  $N_s = 1$ ) is due to the assumption that each data server is always busy when considering simultaneous voice and data users. In the figure,  $N_d$  corresponding to  $N_s = 0, 1, 2, 3$ , and 4 available data servers are considered.  $N_s = 0$  corresponds to simply voice only service, and the assumption does not overestimate the interference since there are no data users. On the other hand, when

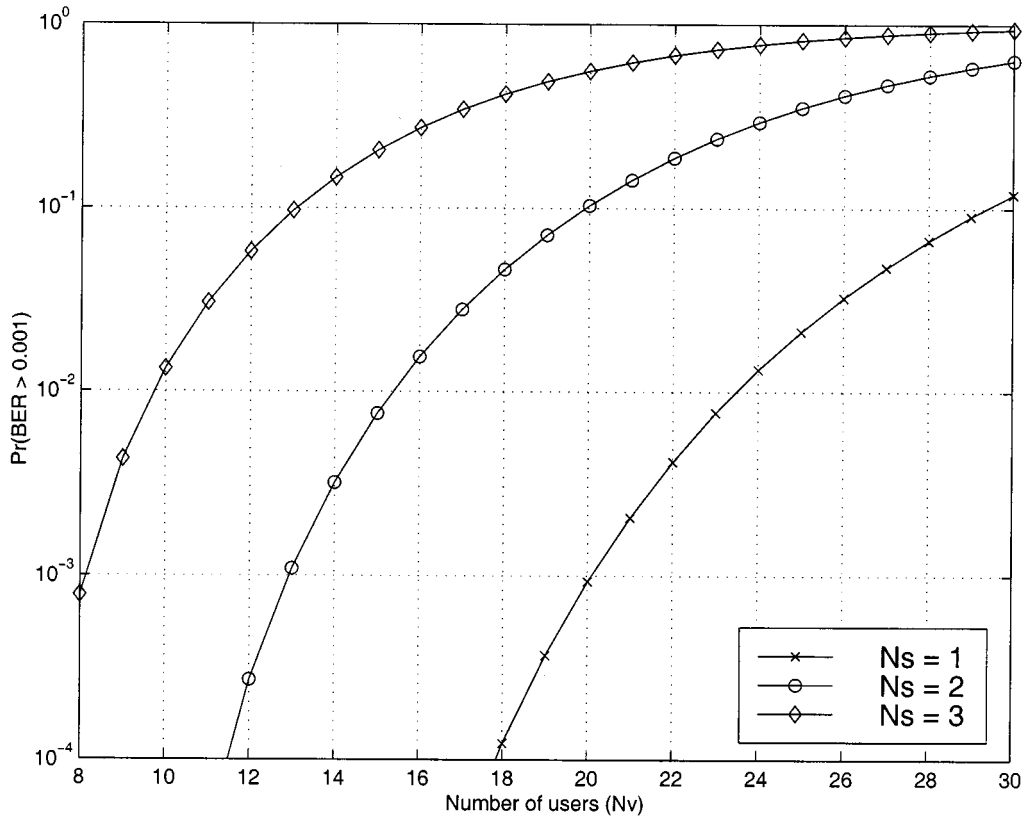


Fig. 14. Outage probability for voice users with perfect power control and no shadowing in a multiple-cell network.

$N_s > 0$ , the assumption overestimates the interference, resulting in a less number of equivalent voice users (i.e., a smaller slope in the curves). Table VII shows the capacity for voice users with perfect and imperfect power control for various values of  $N_s$  and the reduction of overall cell capacity,  $N_c \triangleq N_v + N_d$ , due to imperfect power control. We see that the cell capacity reduction due to power control imperfection remains relatively steady as  $N_s$  increases. The small fluctuations in capacity loss are largely the result of rounding error since voice and data user capacities must be stated as integer values.

In a multiple-cell network with perfect power control and  $N_s$  available data servers, the received  $E_b/I_o$  for a voice user is

$$\left(\frac{E_b}{I_o}\right)_r = \frac{W/R_c}{\left(\left(\sum_{j=1}^{N_v-1} \chi_j\right) + N_s \frac{S_d}{S_v}\right)(1 + F_m) + \frac{\phi}{S_v}} \quad (22)$$

under the assumption that all the data servers are always busy. The outage probability for a voice user is

$$\begin{aligned} \Pr(\text{BER} > 10^{-3}) &= \Pr\left(\left(\frac{E_b}{I_o}\right)_r < \left(\frac{E_b}{I_o}\right)_q\right) \\ &= \Pr\left(\sum_{j=1}^{N_v-1} \chi_j > \delta(N_s)\right) \end{aligned} \quad (23)$$

where

$$\delta(N_s) = \frac{\left(\frac{W/R_c}{\left(\frac{E_b}{I_o}\right)_q} - \frac{\phi}{S_v}\right)}{(1 + F_m)} - \frac{N_s S_d}{S_v}.$$

Fig. 14 shows the outage probability for voice users with perfect power control and no shadowing. With a tolerable outage probability of 1%, the cell capacity is  $N_v = 23, 15, 9$  voice users per

cell for  $N_s = 1, 2, 3$ , respectively. With lognormal shadowing, the cell capacity is  $N_v = 21, 15$ , and 8 correspondingly.

Fig. 15 shows the outage probability for voice users using the proposed power control algorithm with  $N_s = 1$  and no shadowing based on simulation with 400 voice packets. We see that power control imperfections reduce the cell capacity to 19 voice users. Table VIII summarizes the simulation results of the cell capacity for voice users with various values of  $N_s$ . Table IX shows the cell capacity  $N_c$  and the loss due to imperfect power control. We see that the capacity loss is approximately constant as  $N_s$  increases.

2) *Multimedia Sources*: With one video source (user 1),  $N_s$  data servers, and perfect power control, the interference seen by a voice user during the transmission of video frame  $l$  is

$$I(N_s, l) = \left(\sum_{j=1}^{N_v} \chi_j\right) S_v + N_s S_d + c_{1,l} S_{vd} + \phi. \quad (24)$$

The received  $E_b/I_o$  is

$$\left(\frac{E_b}{I_o}\right)_r(l) = \frac{W/R_c}{\left(\sum_{j=1}^{N_v-1} \chi_j\right) + \frac{N_s S_d}{S_v} + \frac{c_{1,l} S_{vd}}{S_v} + \frac{\phi}{S_v}}. \quad (25)$$

and the outage probability for a voice user is

$$\Pr(\text{BER} > 10^{-3}) = \Pr\left(\sum_{j=1}^{N_v-1} \chi_j > \delta(N_s, l)\right) \quad (26)$$

where

$$\delta(N_s, l) = \frac{W/R_c}{\left(\frac{E_b}{I_o}\right)_q} - \frac{N_s S_d}{S_v} - \frac{c_{1,l} S_{vd}}{S_v} - \frac{\phi}{S_v}.$$

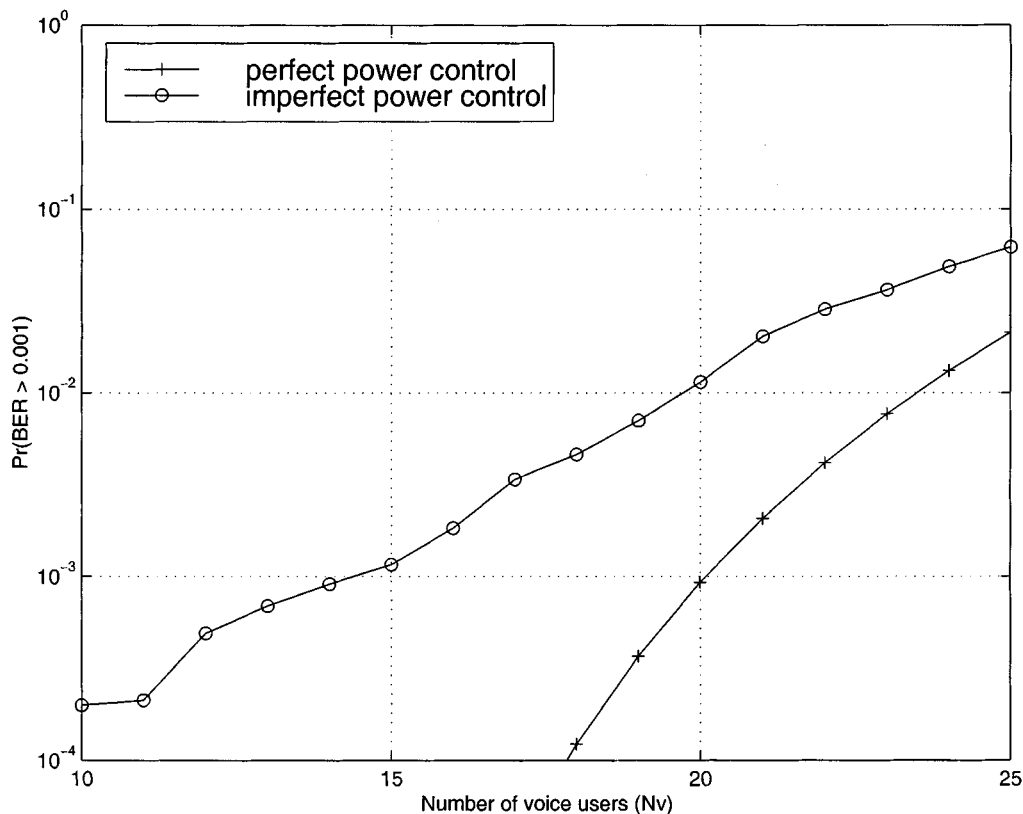


Fig. 15. Outage probability for voice users with  $N_s = 1$  data server and no shadowing in a multiple-cell network.

TABLE VIII  
MAXIMUM NUMBER OF VOICE USERS PER CELL IN A MULTIPLE-CELL NETWORK

$N_s$	$N_d$	no shadowing		log-normal shadowing	
		$N_v$ (perfect)	$N_v$ (imperfect)	$N_v$ (perfect)	$N_v$ (imperfect)
0	0	30	27	30	26
1	5	23	19	21	18
2	18	15	11	15	10
3	32	9	4	8	3

TABLE IX  
TOTAL CELL CAPACITY  $N_c$  IN A MULTIPLE-CELL NETWORK

$N_s$	no shadowing			log-normal shadowing		
	$N_c$ (perfect)	$N_c$ (imperfect)	Loss	$N_c$ (perfect)	$N_c$ (imperfect)	Loss
0	30	27	10.0%	30	26	13.3%
1	28	24	14.3%	26	23	11.5%
2	33	29	12.1%	33	28	15.2%
3	41	36	12.2%	40	35	12.5%

With an  $(E_b/I_o)_q$  of 7 dB for voice users and 13.2 dB for data users, the ratio  $S_{vd}/S_v$  is 4.169. Through simulation performed over 400 voice packets, the cell capacity is 16 voice users with  $N_s = 1$  and an outage probability of 1%. With  $N_s = 2$ , the cell capacity reduces to eight voice users. Using the actual power control, the capacity is 11 voice users with one data server and two voice users with two data servers. Table X gives a summary of the cell capacity under various traffic configurations.

In a multiple-cell network, with  $N_s$  data servers and one video source in each cell, the received  $E_b/I_o$  for a voice user with

perfect power control during the transmission of video frame  $l$  is

$$\left(\frac{E_b}{I_o}\right)_r(l) = \frac{W/R_c}{\left(\left(\sum_{j=1}^{N_v-1} \chi_j\right) + N_s \frac{S_d}{S_v} + c_{1,l} \frac{S_{vd}}{S_v}\right) (1 + F_m) + \frac{\phi}{S_v}} \quad (27)$$

TABLE X  
CELL CAPACITY FOR MULTIMEDIA TRAFFIC USING THE PROPOSED POWER CONTROL ALGORITHM IN A SINGLE-CELL NETWORK

Configuration	$N_v$	$N_d$	$N_{vd}$
Voice only	41	0	0
Data only	0	106	0
Video only	0	0	2
Voice and Data ( $N_s = 3$ )	17	32	0
Voice and Video ( $N_{vd} = 1$ )	19	0	1
Voice, Data, Video ( $N_s = 1, N_{vd} = 1$ )	11	5	1

TABLE XI  
CELL CAPACITY FOR MULTIMEDIA TRAFFIC USING THE PROPOSED POWER CONTROL ALGORITHM IN A MULTIPLE-CELL NETWORK

Configuration	no shadowing			log-normal		
	$N_v$	$N_d$	$N_{vd}$	$N_v$	$N_d$	$N_{vd}$
Voice only	27	0	0	26	0	0
Data only	0	76	0	0	76	0
Video only	0	0	1	0	0	1
Voice and Data ( $N_s = 2$ )	11	18	0	10	18	0
Voice and Video ( $N_{vd} = 1$ )	4	0	1	3	0	1
Data and Video ( $N_s = 1, N_{vd} = 1$ )	0	5	1	0	5	1

and the outage probability for a voice user is

$$\Pr(\text{BER} > 10^{-3}) = \Pr\left(\sum_{j=1}^{N_v-1} \chi_j > \delta(N_s, l)\right) \quad (28)$$

where

$$\delta(N_s, l) = \frac{W/R_c}{(E_b/I_o)_q} - \frac{\phi}{S_v} - N_s \frac{S_d}{S_v} - c_{1,l} \frac{S_{vd}}{S_v}.$$

Through simulation with perfect power control over a sample of 400 voice packets, one data server and one video user, the cell capacity is  $N_v = 4$  with no shadowing and  $N_v = 3$  with lognormal shadowing. With actual power control, simulation results show that the network cannot support any voice users. Table XI summarizes the actual cell capacity for various configurations.

The capacity analysis presented in this section is based on the path-loss exponent  $\beta = 4$  and the intercell interference correction factor  $F_m = 0.44$  in the case of no shadowing and 0.49 in the case of shadowing with standard deviation  $\sigma = 5$  dB. In reality, it is possible that  $\beta < 4$  and/or  $\sigma > 5$  dB for an indoor environment, resulting in higher intercell interference [20]. Therefore, the results of the capacity analysis for the multiple-cell systems may be optimistic depending on the propagation environment.

## V. CONCLUSION

A packetized DS-CDMA system model capable of providing multimedia services has been proposed. The system supports CBR voice, VBR data, and VBR video traffic in a protocol compatible with ATM. Wireless packets have a fixed payload of 24 bytes, thus, two wireless packets constitute one ATM packet. Convolutional coding is used for voice packets, BCH coding

for data (with an ARQ protocol) and video packets. A power control algorithm is proposed for the reverse link, which combines channel estimation with closed-loop power control. A 1-b power command is used for data sources and a 2-b command for voice and video sources. Computer simulation results demonstrate that the proposed power control algorithm outperforms open-loop and closed-loop power control, and the power control using channel estimation. Furthermore, the proposed algorithm has the advantage that the power control error does not increase with the delay between the end of transmission of one packet and the beginning of the next packet. Therefore, it is suitable for packetized transmission and bursty data traffic. The cell capacity under various traffic configurations has been studied for a single-cell network under the assumption of perfect power control. The effect of power control imperfection using the proposed power control algorithm on the cell capacity has been investigated based on computer simulation. The cell capacity analysis has also been extended to a multiple-cell network.

## ACKNOWLEDGMENT

The authors wish to thank the anonymous reviewers for their helpful reviews and suggestions which improved the quality and presentation of this paper.

## REFERENCES

- [1] N. D. Wilson, R. Ganesh, K. Joseph, and D. Raychaudhuri, "Packet CDMA versus dynamic TDMA for multiple access in an integrated voice/data PCN," *IEEE J. Select. Areas Commun.*, vol. 11, pp. 870–884, Aug. 1993.
- [2] M. J. McTiffin, A. P. Hulbert, T. J. Ketseoglou, W. Heimsch, and G. Crisp, "Mobile access to an ATM network using a CDMA air interface," *IEEE J. Select. Areas Commun.*, vol. 12, pp. 900–908, June 1994.
- [3] C.-L. I and K. Sabnani, "Variable spreading gain CDMA with adaptive control for true packet switching wireless network," in *Proc. ICC 1995*, pp. 725–730.
- [4] A. Sampath, P. S. Kumar, and J. M. Holtzman, "Power control and resource management for a multimedia CDMA wireless system," in *Proc. PMIRC 1995*, pp. 21–25.
- [5] J. T.-H. Wu and E. Geraniotis, "Power control in multi-media CDMA networks," in *Proc. VTC 1995*, pp. 789–793.
- [6] Z. Liu and M. El Zarki, "Performance analysis of DS-CDMA with slotted ALOHA random access for packet PCNs," *Wireless Networks*, vol. 1, pp. 1–16, Feb. 1995.
- [7] M. Soroushnejad and E. Geraniotis, "Multi-access strategies for an integrated voice/data CDMA packet radio network," *IEEE Trans. Commun.*, vol. 43, pp. 934–945, Feb. 1995.
- [8] J. Q. Chak and W. Zhuang, "Capacity analysis for connection admission control in indoor multimedia CDMA wireless communications," *Wireless Personal Commun.*, vol. 12, pp. 269–282, March 2000.
- [9] D. Raychaudhuri and N. D. Wilson, "ATM-based transport architecture for multiservices wireless personal communication networks," *IEEE J. Select. Areas Commun.*, vol. 12, pp. 1401–1414, Oct. 1994.
- [10] W. Zhuang, "Integrated error control and power control for DS-CDMA multimedia wireless communications," *Proc. Inst. Elect. Eng.*, vol. 146, pp. 359–365, Dec. 1999.
- [11] S. G. Wilson, *Digital Modulation and Coding*. Englewood Cliffs, NJ: Prentice-Hall, 1996, ch. 5.
- [12] J. G. Proakis, *Digital Communications*, 2nd ed. New York: McGraw-Hill, 1989.
- [13] K. S. Gilhousen, I. M. Jacobs, R. Padovani, A. J. Viterbi, L. A. Weaver, and C. E. Wheatley III, "On the capacity of a cellular CDMA system," *IEEE Trans. Veh. Technol.*, vol. 40, pp. 472–480, May 1991.
- [14] S. Ariyavisitakul and L. F. Chang, "Signal and interference statistics of a CDMA system with feedback power control," *IEEE Trans. Commun.*, vol. 41, pp. 1626–1634, Nov. 1993.
- [15] W. C. Jakes, Ed., *Microwave Mobile Communications*. New York: Wiley, 1974.

- [16] T. S. Rappaport, S. Y. Seidel, and K. Takamizawa, "Statistical channel impulse response models for factory and open plan building radio communication system design," *IEEE Trans. Commun.*, vol. 39, pp. 794–806, May 1991.
- [17] M. G. Jansen and R. Prasad, "Capacity, throughput, and delay analysis of a cellular DS CDMA system with imperfect power control and imperfect sectorization," *IEEE Trans. Veh. Technol.*, vol. 44, pp. 67–74, Feb. 1995.
- [18] *An Overview of the Application of Code Division Multiple Access (CDMA) to Digital Cellular Systems and Personal Cellular Networks*, Qualcomm, Inc., May 1992.
- [19] R. Prasad, A. Kegel, and M. G. Jansen, "Effect of imperfect power control on cellular code division multiple access system," *IEE Elect. Lett.*, vol. 28, pp. 848–849, Apr. 23, 1993.
- [20] A. J. Viterbi, A. M. Viterbi, and E. Zehavi, "Other-cell interference in cellular power-controlled CDMA," *IEEE Trans. Commun.*, vol. 42, pp. 1501–1504, Feb./Mar./Apr. 1994.
- [21] L. Hanzo and J. Streit, "Adaptive low-rate wireless videophone schemes," *IEEE Trans. Circuits Syst. Video Technol.*, vol. 5, pp. 305–318, Aug. 1995.
- [22] P. Mermelstein, A. Jalali, and H. Leib, "Integrated services on wireless multiple access networks," in *Proc. ICC 1993*, pp. 863–867.
- [23] M. Nomura, T. Fujii, and N. Ohta, "Basic characteristics of variable rate video coding in ATM environment," *IEEE J. Select. Areas Commun.*, vol. 7, pp. 752–760, June 1989.



**Salim Manji** (S'95) received the B.A.Sc. and M.A.Sc. degrees in electrical engineering from the University of Waterloo, Waterloo, Canada, in 1995 and 1996, respectively. He is currently working toward the Ph.D. degree at WINLAB, Rutgers, the State University of New Jersey, Piscataway.

During the summers of 1997–1999, he held an internship position with the Wireless Applications Laboratory, Lucent Technologies, Bell Labs, Whippany, NJ. His current research interest is in the area of image transmission over wireless channels.



**Weihua Zhuang** (M'93) received the B.Sc. and M.Sc. degrees from Dalian Marine University, China, in 1982 and 1985, respectively, and the Ph.D. degree from the University of New Brunswick, Canada, in 1993, all in electrical engineering.

Since 1993, she has been a Faculty Member at the University of Waterloo, Waterloo, Ont., Canada, where she is currently an Associate Professor in the Department of Electrical and Computer Engineering. Her research interests include digital transmission over fading dispersive channels and wireless networks for multimedia personal communications.

Dr. Zhuang is a licensed Professional Engineer in the Province of Ontario, Canada.